

1 Progress in the Analysis of Complex Atmospheric Particles

2 Alexander Laskin,^{1,*} Mary K. Gilles,² Daniel A. Knopf,³ Bingbing Wang,¹ Swarup China¹

3 ¹*Environmental Molecular Sciences Laboratory, Pacific Northwest National Laboratory,*
4 *Richland, Washington, USA.*

5 ²*Chemical Sciences Division, Lawrence Berkeley National Laboratory, Berkeley, California, USA.*

6 ³*Institute for Terrestrial and Planetary Atmospheres, School of Marine and Atmospheric*
7 *Sciences, Stony Brook University, Stony Brook, New York, USA.*

8 *corresponding author. Email: *alexander.laskin@pnnl.gov*

9 TABLE OF CONTENT

10	Abstract	2
11	1. Introduction.....	3
12	2. Multimodal Chemical Characterization of Particles	4
13	2.1. Chemical Imaging Techniques.	4
14	2.2. Atmospheric Transformations of Particles	6
15	2.3. Molecular-level Characterization.....	9
16	3. Exchange of Chemical Constituents at Air-Surface Interfaces.....	11
17	3.1. Wind Blown Dust	11
18	3.2. Air-Surface Interfaces of Biological Particles	14
19	3.3. Sea Spray Aerosol	16
20	3.4. Airborne Soil Organic Particles	18
21	4. Summary.....	21
22	5. Disclosure Statement.....	22
23	6. Acknowledgements	22
24	7. Literature Cited.....	28

25
26 **Keywords:** Aerosol, Chemical Imaging, Molecular-level, Multi-Phase Chemistry, Atmospheric Aging,
27 Environmental Interfaces

28

29 Manuscript in preparation for *Annual Reviews in Analytical Chemistry*

30 **Abstract**

31

32 This manuscript presents an overview on recent advances in field and laboratory studies of
33 atmospheric particles formed in processes of environmental air-surfaces interactions. The
34 overarching goal of these studies is to advance predictive understanding of atmospheric
35 particle composition, particle chemistry during aging, and their environmental impacts. The
36 diversity between chemical constituents and lateral heterogeneity within individual particles
37 adds to the chemical complexity of particles and their surfaces. Once emitted, particles undergo
38 transformation via atmospheric aging processes that further modify their complex composition.
39 We highlight a range of modern analytical approaches that enable multi-modal chemical
40 characterization of particles with both molecular and lateral specificity. When combined, they
41 provide a comprehensive arsenal of tools for understanding the nature of particles at air-
42 surface interactions and their reactivity and transformations with atmospheric aging. We
43 discuss applications of these novel approaches in recent studies and highlight additional
44 research areas to explore environmental effects of air-surface interactions.

45

46 1. Introduction

47 Atmospheric aerosols are complex multi-phase chemical systems composed of a myriad of
48 components from both natural (sea spray, dust storms, pollen, biological particle discharge,
49 biogenic emissions of organic particles, etc.) and anthropogenic (combustion related emissions
50 from industry and transportation) sources. They can be either directly emitted (primary
51 aerosols) or formed by gas-to-particle conversion processes (secondary aerosols). In many
52 locations, primary and secondary aerosol components are mixed within individual particles
53 (internal mixing) and between separate particles (external mixing). These result from
54 components exchanging between different aerosol phases during atmospheric aging and
55 transport.(1) Aerosols impact profoundly a number of environmental issues such as radiative
56 forcing of the Earth's climate,(2) air quality(3), visibility,(4) public health and toxicology,(5)
57 biogeochemical cycles,(6) and nutrient transport in natural ecosystems.(7) Despite their
58 acknowledged importance, our understanding of complex multiphase chemistry of atmospheric
59 aerosols remains insufficient to quantitatively predict their role in the atmospheric
60 environment. The inherent complexity of aerosols requires developments and novel
61 applications in analytical chemistry to characterize particle composition, morphology, phase
62 and internal structures, their transformations through multi-phase chemistry of atmospheric
63 aging, and the associated consequences on cloud-nucleating propensity and optical properties.

64 The field of aerosol analytical chemistry has been substantially advanced over the last two
65 decades, as summarized in comprehensive review manuscripts(8-16) and book chapters(17; 18)
66 that feature developments of state-of-the-art instruments and methodologies for online and
67 offline aerosol characterization. Advantages of online mass spectrometry and optical
68 spectroscopy techniques are the ability to probe aerosolized materials with high temporal
69 resolution enabling in-situ studies of particle size and composition, and following
70 transformations as they occur in real-world field studies, test facilities, and environmental
71 chambers. Offline techniques applied to particle samples, and their unique advances fall within
72 chemical imaging of individual particles and molecular-level speciation of complex organic
73 constituents in bulk particle samples. Offline techniques also offer the practical advantage of
74 the option for correlative multi-modal characterization of particles samples.

75 This paper highlights recent advances in aerosol chemistry revealed by offline methods
76 used to study air-surface interactions and processing where environmental particles containing
77 surface components are ejected into the atmosphere. Currently, the mechanisms and
78 atmospheric impacts of such processes lie at the forefront of aerosol research.

79

2. Multimodal Chemical Characterization of Particles

80 Data on chemical composition, size, morphology, internal mixing, and phase states of
81 particles obtained by offline analysis methods are crucial for understanding aerosol formation
82 and reaction mechanisms, their atmospheric evolution, and their impacts and source
83 apportionment. However, acquiring comprehensive information on the chemical composition
84 of atmospheric particles is challenging because no single analytical chemistry technique can
85 provide all the information required. For example, electron and X-ray microscopies elucidate
86 morphology and internal structure at the nanometer scale.(19-21) However, in the case of
87 electron microscopy, chemical information is limited to elemental composition of particles,
88 while the nature of elemental chemical bonding can be inferred from X-ray microscopy. Mass
89 spectrometry techniques, assisted with novel ambient pressure ionization/substrate sampling
90 sources, enable detailed molecular-level characterization of individual constituents of organic
91 particles (at the expense of spatial resolution).(8; 11; 16) As a result, comprehensive
92 characterization of atmospheric particles typically requires combining analytical methods to
93 yield complementary information ranging from microscopic properties of individual particles to
94 advanced chemical characterization of the complex molecules they are composed of. A variety
95 of microscopy, microprobe, spectroscopy and mass spectrometry techniques are commonly
96 applied to characterize the size, morphology, phase and composition of particles collected in
97 field campaigns and laboratory studies.(8; 10; 11; 16; 21; 22) Typically, information from one
98 analytical technique guides further measurements and laboratory studies. Below we describe
99 how qualitative and quantitative information obtained from these studies is essential for
100 evaluating optical properties of particles, understanding their aging, reactivity, hygroscopicity
101 and cloud-forming propensity.

102

2.1. Chemical Imaging Techniques.

104 Applications of microscopy, micro-spectroscopy, and imaging mass spectrometry
105 techniques (i.e., CCSEM/EDX, ESEM, FIB/SEM, HRTEM/EELS, STXM/NEXAFS, TOF-SIMS, nano-
106 SIMS, micro-FTIR and micro-Raman spectroscopy) have focused on aspects of multi-phase
107 atmospheric chemistry and physics using chemical imaging (elemental and molecular group
108 mapping) of field and laboratory particle samples. Recent literature (2012-2015) includes a
109 broad range of topics such as: particle type assessments in field and test facility studies based
110 on their composition and mixing states,(23-34) particle transformations due to atmospheric
111 aging processes in field(23; 26; 35-38) and simulated laboratory experiments,(39-43) in-situ
112 observations of phase transitions(44-47) and liquid-liquid phase separation(48-51) in hydrated
113 particles, depth-profiling(52) and cross-sectioning(53-55) examination of particle internal
114 composition, assessment of particles ice nucleation propensity(56-61) and optical
115 properties(62-64) inferred from chemical imaging observations, and understanding the kinetics

116 and mechanisms of atmospheric aging processes based on the isotope ratio measurements(65;
117 66) on individual particles.

118 SEM and TEM coupled to EDX microanalysis are commonly used for analysis of particle
119 morphology, size, elemental composition, and internal structures with nanometer (SEM) and
120 sub-nanometer (TEM) lateral resolution.(19; 21) Operation of SEM in computer-controlled
121 mode (CCSEM) permits routine analysis of hundreds-to-thousands of particles deposited on
122 substrates, and provides statistically significant data on particle-type populations. TEM is used
123 for more narrowly focused studies on particle internal composition and mixing state. EELS
124 coupled to TEM enables assessment of chemical bonding for selected elements within
125 individual particles. Crystalline structures of crustal particles can be determined through
126 analysis of the selected-area electron diffraction. Although conventional SEM and TEM require
127 vacuum environments, chambers and sample holders have been developed that allow exposure
128 of particles to a few Torr of residual gas during imaging, i.e. environmental operation (ESEM
129 and ETEM, respectively). Using water vapor, ESEM and ETEM allow real time imaging of
130 hygroscopic transformations over the entire range of relative humidity (RH from 1 to 100%).
131 Finally, novel dual beam FIB/SEM instruments have been applied for cross-sectioning and
132 chemical imaging of particle interiors.

133 Synchrotron-based soft X-ray microscopes (STXM/NEXAFS) enable chemical imaging of
134 particles with advanced speciation of carbon bonding and chemical characterization of different
135 forms of organic material.(20) STXM has lower lateral resolution (>20 nm) than SEM and TEM,
136 but its higher chemical specificity has made it an instrument of choice for analysis of organic
137 and mixed organic/inorganic particles. Chemical bonding and oxidation states of other common
138 elements in atmospheric particles (e.g. N, O, S, Fe, etc.) can be also investigated, depending on
139 the specific STXM instrument. Selected features of NEXAFS spectra, indicative of specific
140 element functionalities are used to construct particle component maps, grouping and
141 assessment of particle-types and their mixing states.(67) Similar to ESEM and ETEM, recently
142 developed environmental sample holders(68; 69) enabled studies of particle hygroscopic
143 transformations(51; 70) providing chemical imaging specificity of liquid-liquid phase
144 separation.(48)

145 SIMS instruments operate in vacuum and interrogate solid samples using a primary ion
146 beam and collecting secondary ions ejected from the sample.(71) Using a TOF mass analyzer, a
147 signature mass spectrum with lateral resolution of a few nanometers is obtained. If a low
148 primary ion dose is used, analysis is limited to the outermost layers of particles.(72) Whereas a
149 higher current primary ion beam allows depth profiling of chemical stratification within
150 particles.(73; 74) Nano-SIMS instruments detect simultaneously a limited number of selected
151 ions (up to seven), but with the higher mass resolution necessary for quantitative analysis of
152 isotopic fractionation of elements contained in particles. This isotopic analysis can provide
153 fundamental insights into sources and the atmospheric history of particles.(66; 75)

154 Raman and FTIR spectrometers are complimentary methods because vibrational modes that
155 are not allowed in the IR may be Raman active.(76) When interfaced with optical microscopes,
156 they allow chemical imaging of micrometer size particles(77; 78) and in-situ monitoring of
157 spectral bands correlated with physicochemical transformations of particles.(58-60; 74) Using
158 specially designed sample holders and flow reactor assemblies, measurements of water uptake
159 by particles, their subsequent phase transformations and ice nucleation of ice can be
160 quantified.

161 Due to their chemical complexity, many studies employ multi-modal combinations of the
162 chemical imaging techniques to unravel the complex multiphase particle chemistry.

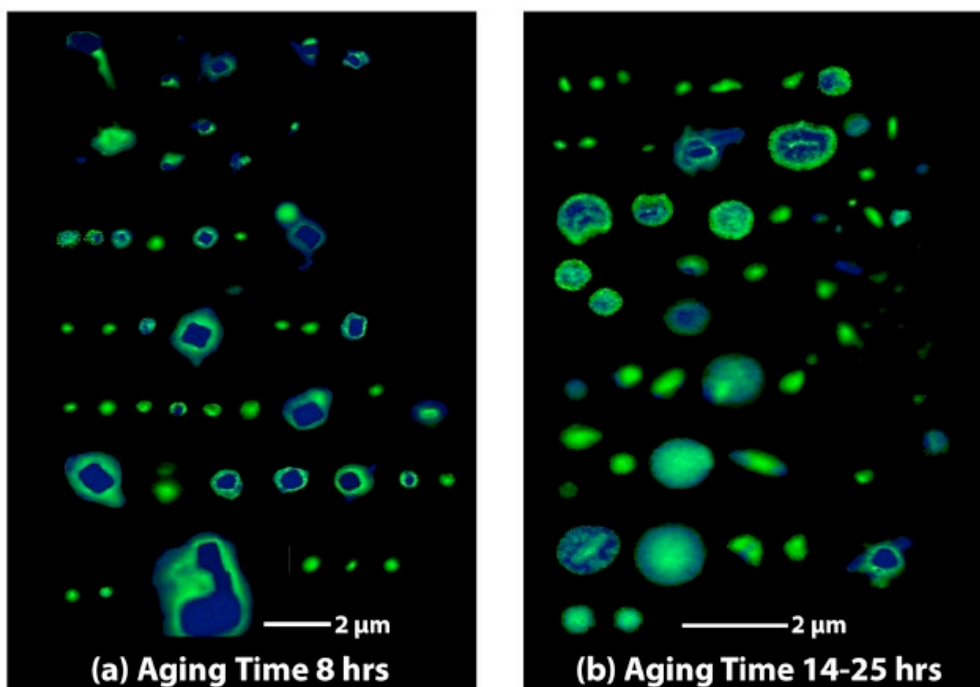
163

164 **2.2. Atmospheric Transformations of Particles**

165 Understanding aerosol effects on the environment and climate requires an adequate
166 description of particle physicochemical properties at their emission source and predictive
167 understanding of their consequent atmospheric transformations (that are yet insufficiently
168 understood for many types of aerosols). Processes of multiphase reaction chemistry,
169 segregation of different components within individual particles, uptake of gaseous species,
170 coagulation, modifications of particle morphology, etc. – all have profound impacts on particle
171 hygroscopic and optical properties, viscosity and mixing state, reactivity and propensity to serve
172 as CCN and IN.

173 Chemical imaging approaches are used to elucidate transformations of specific particle
174 types collected in field and laboratory studies. Mechanisms are usually inferred from field
175 observations, which in turn guide follow-up laboratory studies designed to test a hypothesis.
176 Figure 1 compares STXM maps of relatively fresh and aged marine particles collected onboard
177 research aircraft in central California. Particle regions enriched in organic acids are shown in
178 green, and inorganic (mostly NaCl) components are shown in blue.(26) The maps indicate
179 morphology and internal composition changes due to in-particle reactions between organic
180 acids and NaCl components, as confirmed by laboratory studies.(39; 40) Complementary
181 multimodal STXM, CCSEM/EDX and micro-FTIR techniques showed that particles containing sea
182 salt and weak organic acids undergo irreversible transformations through multi-phase
183 chemistry driven by acid-displacement reactions and subsequent degassing of volatile products
184 HCl or HNO₃ products. These chemical reactions are accelerated by particle dehydration cycling
185 and result in changes in particle viscosity, hygroscopicity, phase transitions and separations,
186 and thereby modify particle environmental impacts and lifecycle.(44; 79; 80)

187



188
 189 **Figure 1.** STXM maps of particles of a marine origin with different transport (and hence, aging) times
 190 from the CARES 2010 field study.⁽⁸¹⁾ Areas dominated by organic carbon are green, and inorganic
 191 components are blue. (Reproduced with permission from reference (26). Copyright 2012 Wiley-
 192 Blackwell).

193
 194 The complementary combination of STXM/NEXAFS and CCSEM/EDX chemical imaging data
 195 sets has also provided a quantitative assessment of mixing states of carbonaceous particles
 196 aged in the photochemical environment of urban plume.^(23; 24) STXM provided experimental
 197 visualization of how soot and organic carbon constituents were mixed within individual
 198 particles and CCSEM provided corresponding information on the inorganic content. Combined,
 199 this unique study provided a quantitative assessment of the particle-type classes,⁽²³⁾ and
 200 individual particle characteristics such as the particle-specific diversity, bulk population
 201 diversity, and mixing state index determined for particles with different atmospheric aging
 202 history.⁽²⁴⁾ It showed that the mixing states of urban particles in the Sacramento, CA region
 203 were driven by local emissions of black carbon-containing particles that were coated by
 204 products from gas phase secondary chemistry and/or coagulated with sea spray, sulfate, and
 205 organic particles originating from refineries in the San Francisco Bay region. These unique
 206 results provided the first quantitative description of particle mixing state changes during
 207 transport parameterized for use in atmospheric modeling simulations. This allows additional
 208 model refinement based on the results of the multi-modal chemical imaging of particles.

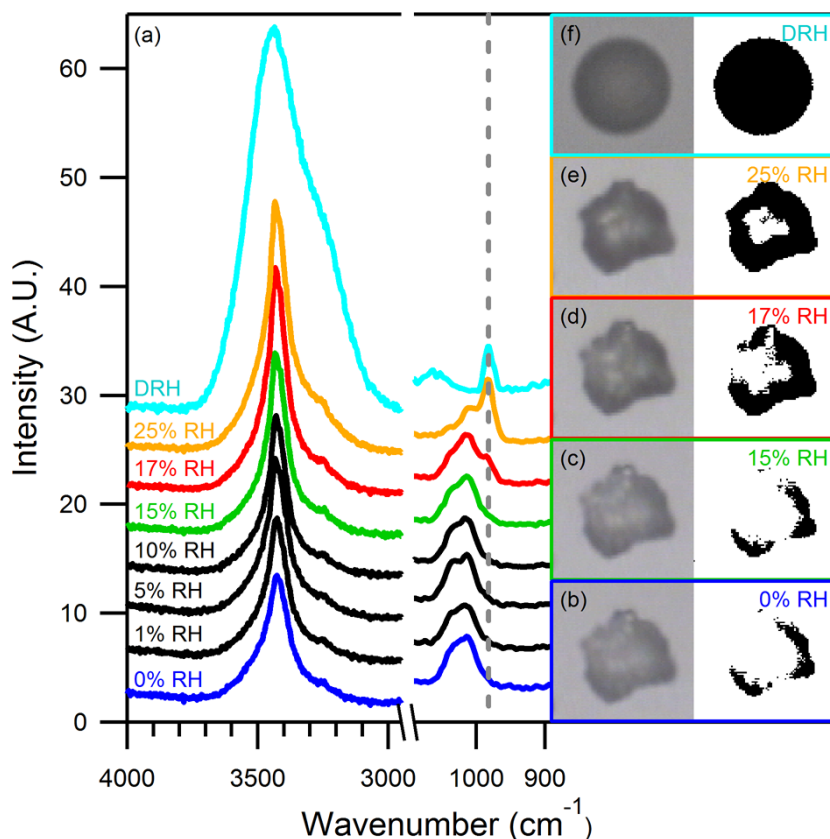
209 Increasingly, chemical imaging methods are used for dynamic in-situ laboratory studies that
 210 simulate the atmospheric particle life cycles using specially designed micro-reactors. Elucidating

211 the effects of particle composition and their transformations on processes governing cloud
212 microphysics, such as hygroscopic growth, phase transitions, and nucleation of cloud droplets
213 and ice crystals is of particular interest. ESEM and ETEM studies have advanced our
214 understanding of the hygroscopic behavior of individual particles composed of inorganic salts
215 and their mixtures.(19) Microscopic observations with high (nano-meter) lateral resolution
216 allow direct detection and visualization of multistep phase transitions and separations -
217 processes that are not easily probed by other techniques. However, electron microscopies do
218 not allow simultaneous chemical analysis while particles undergo hygroscopic transformations.
219 Instead, Electron microprobe techniques are done under high vacuum (dry conditions of
220 particles) and also typically cannot distinguish between organic constituents in particles.
221 Complementary STXM/NEXAFS observations provide chemical bonding specificity, albeit at
222 lower lateral resolution than ESEM and ETEM.(48; 82) One recent example of dynamic chemical
223 imaging was performed on particles containing ammonium sulfate and organic carbon
224 components. STXM maps showed that even in fully deliquesced particles organic and inorganic
225 liquid components were notably separated with the organic components enriched in the outer
226 layer.(48) During dehydration experiment, STXM/NEXAFS was used to determine the
227 contributions of each component in the liquid phases and to monitor dynamics of liquid-liquid
228 phase separations. It has been observed that both liquid phases contained inorganic and
229 organic components, while their fractionation between the phases gradually increased at lower
230 RH. Other study showed that multiple solid and liquid phases appear along with changes in the
231 microstructures of field collected particles during relative humidity cycling.(51) A recent multi-
232 modal study included STXM/NEXAFS characterization of field collected particles for quantifying
233 C, N, and O, followed by in situ chemical imaging of water uptake by particles, which in turn was
234 followed by SEM/EDX microanalysis of dry particles. From analysis of NEXAFS spectra recorded
235 for individual particles during hydration the mass of water absorbed by each individual particle
236 was quantified. Combining the STXM/NEXAFS and SEM/EDX data sets allowed determination of
237 mass-based hygroscopicity parameters for field collected atmospheric particles.(82)

238 Additional characterization of particle organic material can be achieved using micro-Raman
239 spectroscopy. This method integrates Raman scattering spectrometry with an optical
240 microscope to allow spectra acquisition from microscopic samples. Micro-Raman analysis is
241 performed at substantially lower lateral resolution (>100 nm) than electron and X-ray methods,
242 but provides complementary chemical information. Figure 2 shows the micro-Raman data set
243 acquired over a ~15 μm multi-component sea salt particle at increasing values of RH.(60)
244 Dynamic transformation is assessed based on the changes in Raman spectra indicative of water
245 uptake and dissolution of sulfates in the outer particle layers. These are exhibited by the
246 increase of hydrate (3400 cm^{-1}) and aqueous sulfate (981 cm^{-1}) peaks. Binary chemical imaging
247 maps that outline locations of dissolved sulfate within interior of the particle were constructed

248 from the peak intensities. To simulate conditions of low-temperature anvil cirrus formation, sea
249 salt particles were imaged in a set of systematic deliquescence and ice nucleation experiments.
250 The observations indicated that fresh and aged sea-salt particles can induce ice crystal
251 formation through both deposition and immersion nucleation modes.(60)

252
253



254
255 **Figure 2.** Raman spectra (a) and optical images (b–e) of an approximately 15 μm mixed sea salt particle
256 captured during water uptake/ice nucleation experiments. Dynamic changes in particle composition
257 corresponding to water uptake and dissolution of sulfate components at the outer particle layers are
258 evidenced by differences in the spectra and the binary maps (right panels). For comparison, a fully
259 deliquesced sea salt particle is shown in (f). (Reproduced with permission from reference (60). Copyright
260 2014 American Chemical Society).

261
262

2.3. Molecular-level Characterization

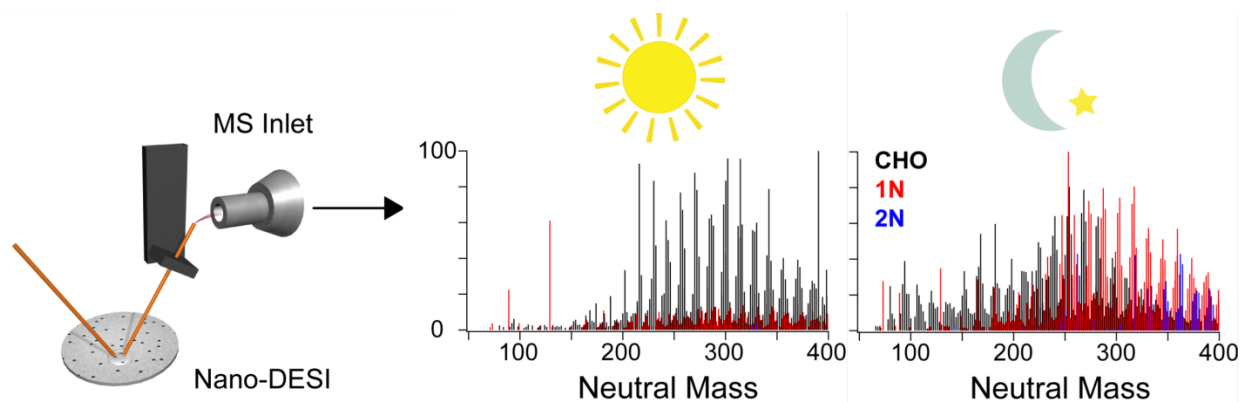
263 Understanding molecular compositions and transformations of complex mixtures of OA
264 components is arguably the most significant challenge in atmospheric aerosol research.
265 Because of its ability to provide molecular-level information, HRMS assisted with ambient
266 pressure surface ionization is uniquely suited for chemical characterization of aerosol samples
267 collected on substrates.(11) For instance, a novel nano-DESI/HRMS approach enables rapid and

268 sensitive (<10 ng) analysis of laboratory and field collected aerosol samples.(83) Nano-DESI
269 enables fast and efficient collection, soft ionization, and analyte transfer that together
270 significantly improve detection limits (compared to other ambient ionization methods). Nano-
271 DESI does not require special sample preparation or pretreatment.(83) Elemental compositions
272 of individual constituents of OA are determined based on high mass resolution and high mass
273 accuracy of the acquired spectra.(16) Their possible molecular structures can be inferred from
274 analysis of fragmentation patterns obtained in MSⁿ experiments.(84; 85) This technique has
275 provided molecular and structural characterization of molecules in field collected OA, including
276 those containing nitrogen,(85-87) sulfur,(85; 88) and various metals.(89) Nano-DESI has also
277 been used in laboratory studies of the molecular transformations of OA relevant to the
278 formation of atmospheric brown carbon.(22)

279 Figure 3 shows a schematic drawing of the nano-DESI technique and the HRMS spectra of
280 ambient OA collected during the 2010 CalNex campaign at Bakersfield, CA.(86) For comparison,
281 characteristic HRMS spectra collected at the daytime and the nighttime are shown.
282 The high fraction of CHO compounds, characteristic for fresh OA produced by photochemistry
283 and ozonolysis, dominate the daytime spectrum. The increased fractions of nitrogen-containing
284 CHON₁₋₂ compounds are evident in the nighttime spectrum. By comparing plausible reactant-
285 product pairs within molecular species identified in the mass spectra, changes in the OA
286 chemical composition between day and night were assessed. Over 50% of the CHON₁₋₂ species
287 had CHO precursor product pairs consistent with imidization reactions and formation of species
288 with –C=N–C=C– chemical bonds (Schiff bases). These reactions involve ammonia and carbonyl
289 groups on the precursor species, and they suggest a potential role of the Schiff bases in forming
290 nitrogen-containing OA.(86) Formation of these low-volatility and potentially light absorbing
291 compounds may play an important role in OA atmospheric transformations that remain poorly
292 understood.

293

294



295
 296 **Figure 3.** Left panel: Schematic of the nano-DESI analysis of organic aerosol. In nano-DESI, the analyte
 297 deposited on a substrate is probed by an online liquid extraction followed by soft nanoelectrospray
 298 ionization. Right plots: Representative nano-DESI mass spectra of samples from Bakersfield, CA collected
 299 during day and night, respectively. The colors correspond to the number of N atoms in the chemical
 300 formula with black = 0 N, red = 1 N, blue = 2 N. (Reproduced with permission from reference (86).
 301 Copyright 2013 Elsevier, Ltd.).

302 **3. Exchange of Chemical Constituents at Air-Surface Interfaces**

303 Although atmospheric aerosol chemistry and physics processes are complex, the
 304 fundamental scientific understanding of aerosols has advanced tremendously over the last two
 305 decades. These advances were based on combinations of field, laboratory, and modeling
 306 studies. For example, just in the past year numerous comprehensive review manuscripts
 307 summarized existing knowledge on aerosol sources, composition, transformations and
 308 impact.(5; 22; 90-94) These reviews also highlighted scientific challenges and future directions
 309 in aerosol research. Recent studies indicate an insufficient understanding of atmospheric
 310 processes involving aerosols that are either directly ejected from environmental surfaces(95;
 311 96) or indirectly controlled by the composition and physicochemical transformations of the
 312 corresponding surfaces.(97) In this particular scientific area, novel methodologies for particle
 313 chemical imaging and molecular-level characterization are essential for providing new
 314 transformational insights and discoveries. The synopsis of this section is not intended as an
 315 inclusive review of environmental processes at air-surface interfaces. Rather, we embrace
 316 selected topics where offline analysis methods are best suited to provide key advances to
 317 examine unrecognized processes of particle ejection and transformation.

318 **3.1. Wind Blown Dust**

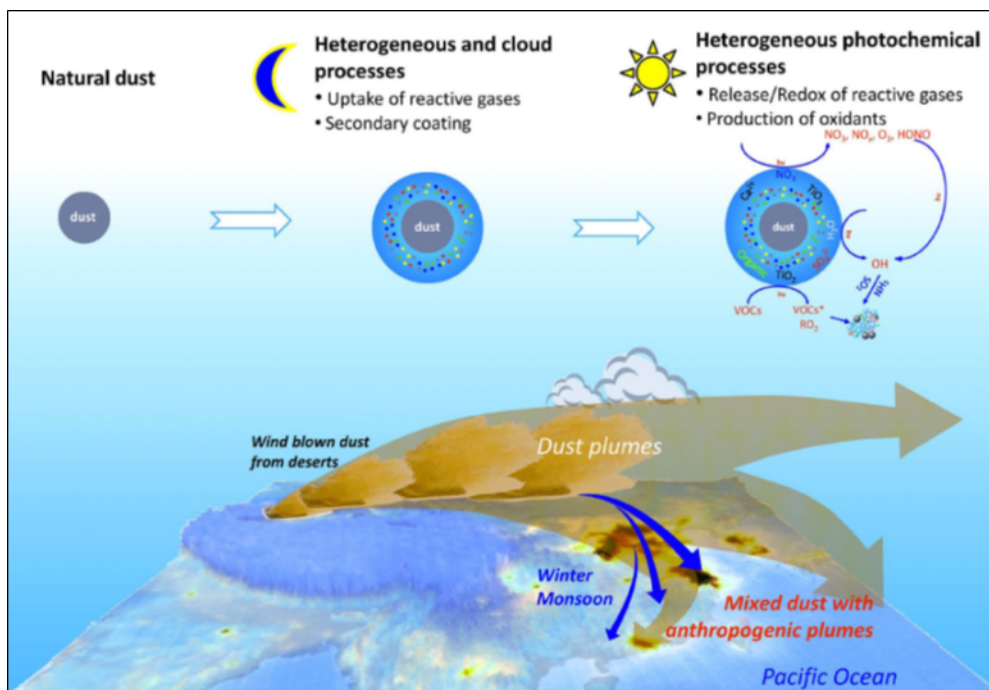
319 Wind-blown mineral dust is one of the major sources of primary atmospheric particles that
 320 affect atmospheric environment and climate through light absorption and scattering, and acting
 321 as either CCN or IN.(98) Atmospheric aging of dust particles, through multiphase chemistry
 322 during their transport and cloud processing, results in their internal mixing with condensed-

323 phase organic constituents that modify particle composition and physical properties. Over the
324 last decades, research efforts focused separately on either mineral dust or OA atmospheric
325 chemistry. These studies provided fundamental knowledge on the atmospheric impact of either
326 dust(98) or OA.(99) However, very few studies examined the effects of condensed organic
327 constituents reacting *with* mineral dust. For example, Fe(III)-rich components of mineral dust
328 can induce a variety of photo-chemical reactions with organic compounds in the presence of
329 sunlight where Fe(III) can act as either a reactant or as a catalyst.(92; 100) These reactions
330 determine the physical properties of mixed "OA/Fe(III)" particles, such as phase state and
331 viscosity, interactions with water, gas-particle partitioning, reactivity, etc. On regional and
332 global scales, reactions of long range transported Fe containing particles are of significant
333 interest because they impact biological productivity of phytoplankton in the oceans and
334 consequently the biogeochemical cycling of sulfur.(101)

335 As discussed in section 2.2., in marine particles, organic acid components of OA can react
336 with inorganic components through multi-phase aqueous chemistry where the reaction
337 equilibrium is shifted to the products by rapid irreversible degassing of volatile products.(26;
338 39; 40) These reactions are common for a broad class of water-soluble organic acids present in
339 both biogenic and anthropogenic OA. Analogous reactions and formation of organic salts are
340 reported for particles containing calcite components of mineral dust.(80; 102) Considering this
341 reactivity for Fe(III)-containing dust components, the organic salts produced would
342 preferentially form on particle outer layers. For instance, the (oxyhydr)oxide surface of
343 hematite can be eroded by carboxylic acids (R-COOH) driven by evaporation of water (a
344 reaction product). The hematite degradation processes may be further enhanced in the
345 presence of UV-Vis radiation because of the unique chelating and photo-catalytic activity of
346 Fe(III). Specifically, chelated [Fe(III) - R-COOH] complexes absorb light in the UV-Vis range and
347 decompose into Fe(II) and \cdot R-COOH pairs.(103) \cdot R-COOH radicals can subsequently decompose
348 into smaller oxygenated organic compounds, CO₂ and peroxides. The radicals may participate in
349 oligomerization processes, while CO₂ and high volatility oxygenated organics can partition into
350 the gas phase. Peroxides can drive Fenton chemistry, Fe(II) to Fe(III) re-oxidation, creating a
351 photo-catalytic cycle in which organic acid components are continuously converted into
352 reactive products, followed by their decomposition and oligomerization reactions. Modeling
353 these photo-catalytic processes suggests they may drive aqueous phase aging of atmospheric
354 organics in the presence of Fe(III), a topic requiring further study.(104)

355 Consistent with the above discussion, multi-phase photochemistry of mixed OA/dust
356 particles may also contribute to new particle formation and growth in dust plumes mixed with
357 anthropogenic pollution. Figure 4 illustrates Asian dust transformation in a context of photo-
358 induced, dust surface-mediated reactions inducing new particle formation as reported in recent
359 field measurements.(97) Complementary to known heterogeneous atmospheric chemistry of
360 dust, the photo-catalytic processes in mixed OA/dust particles may have an additional impact

361 on the environment. Specifically, gas-phase partitioning of volatile oxygenated organics
362 produced through photochemistry in mixed OA/Fe(III) particles may be an unrecognized source
363 of nucleating vapors contributing to new particle formation and growth.
364



365
366
367 **Figure 4.** Schematic Transformations of Asian dust during its atmospheric transport: 1) Fine mineral dust
368 is aerosolized by winds in the remote Gobi desert area, 2) dust particles acquire secondary coatings
369 when transported over industrial regions with anthropogenic pollution, 3) aged dust particles are
370 transported into the Pacific region and experience multi-phase photochemistry that releases reactive
371 gases relevant to new particle formation and growth. (Reproduced with permission from reference (97)
372 Copyright 2014 Nature Publishing Group).

373
374 As a result of the OA/Fe(III) multi-phase chemistry discussed above, multiple changes in
375 particle properties are expected. First, the optical properties of these systems would be altered
376 depending upon different scenarios of atmospheric aging and specific OA composition (e.g.
377 biogenic - less aromatic versus anthropogenic - higher aromatic precursors; chelated Fe(III)-
378 organic complexes are strong chromophores). Second, changes in particle viscosity are
379 expected because of the gas-phase partitioning of CO₂ and volatile organic products on one
380 side, and resulting oligomerization processes on the other side. These factors strongly affect
381 particles' CCN and IN ability. The degree to which these combined processes alter OA
382 composition, particle optical properties, and their CCN and IN ability remain an open question.
383 These questions can be addressed through complementary applications of off-line techniques
384 that probe particle samples collected in field and laboratory studies.

385

386 3.2. Air-Surface Interfaces of Biological Particles

387 Windblown biological particles play a vital role in the Earth's system through various
388 processes at the atmosphere-biosphere interface. During the past decade, biological particles
389 received extensive attention not only because of public health impacts, but also due to their
390 role in climate, atmospheric chemistry and physics.(105-108) Biological particles influence cloud
391 microphysical processes by serving as CCN and IN, thereby affecting the hydrological cycle and
392 Earth's climate. Biological particles are emitted by living organisms directly to the atmosphere
393 and consist of various cellular particles such as pollen, fungal spores, bacteria, viruses,
394 fragments of plants and animals, debris of dead organisms. Atmospheric biological particles can
395 be found in a broad size range, diameters vary from nanometer (e.g., viruses, macromolecules)
396 up to few hundred micrometers (pollens, plant debris).(5; 90) Estimated mass emissions into
397 the atmosphere range from $10\text{-}10^3 \text{ Tg yr}^{-1}$ (109) and they are believed to be the dominant
398 source of organic aerosol in the tropics.(110)

399 Fungal spores are major contributors to biological particles and their emission estimates
400 range between 8 to 186 Tg yr^{-1} .(105; 106; 110) Global model simulations estimated that fungal
401 spores contribute 23% of total primary emissions of organic aerosol in the atmosphere.(110)
402 Plants, vegetation, soils, litter and decaying organic matter are the major sources of fungal
403 spores emitted by active discharge or winds.(105; 110) Several studies suggest that biological
404 particle emissions are linked to atmospheric conditions such as rainfall, relative humidity, winds
405 and thunderstorms, that influence daily variations in the number fluxes.(111-113) Furthermore,
406 these atmospheric conditions trigger emission and deposition of biological particles, thus
407 impacting the microbiome of ecosystems at the Earth surface.(5) Summer rain in boreal and
408 semi-arid forests led to an increase both in biological particle and total particle
409 concentrations.(114) One hypothesis is that fungal spores and other biological particles are
410 lofted from splashing of rain droplets encountering soil and leaf surfaces.(114)

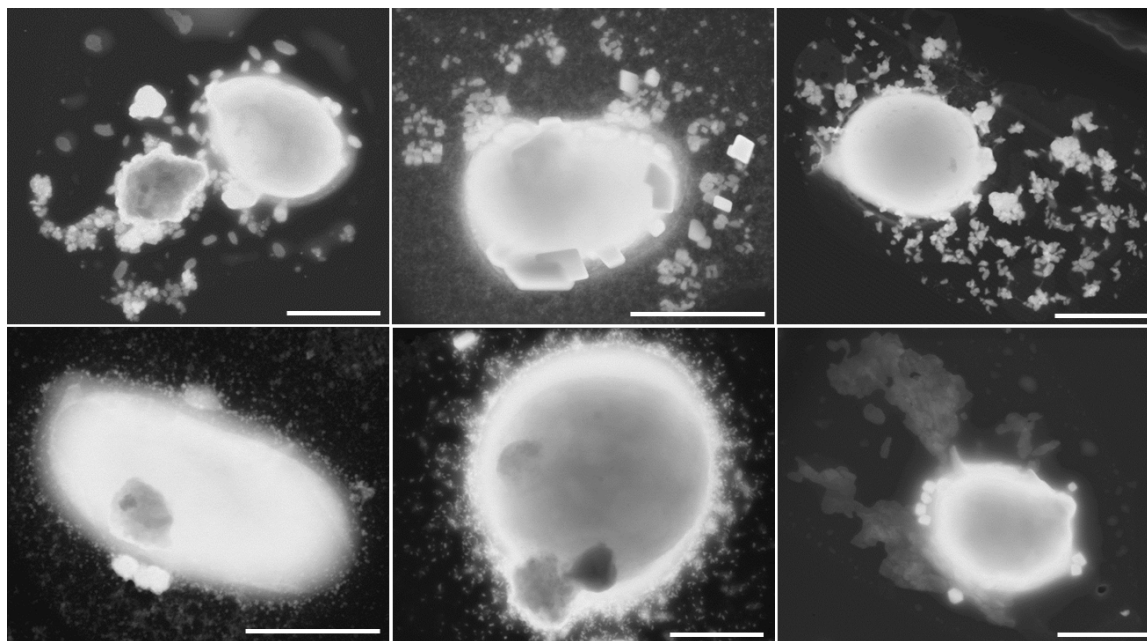
411 Due to their similarities with other carbonaceous particles, measuring and detecting
412 biological particles by in-situ aerosol characterization methods is challenging. This results in
413 ambiguous data on their atmospheric concentrations and chemical composition(115), which
414 produces large uncertainties in estimates of their global budget.(105) Off-line micro-
415 spectroscopy techniques, i.e. electron microscopy, micro-Raman and micro-FTIR spectroscopy,
416 light microscopy and biochemical staining, and autofluorescence based techniques, are
417 exceptionally well suited for detecting and quantifying morphological characteristics and
418 chemical fingerprints of biological particles.(34; 111; 116)

419 Coarse pollen grains attract water below water saturation, can act as CCN and further
420 regulate precipitation by acting as coalescence embryos.(117) However, pollen grains tend to

421 rupture when exposed to high humidity (or hydrate in rainwater), and release cytoplasmic
422 debris and starch grains in the size range from few nanometers to several micrometers.(118;
423 119) Fragmented pollen particles may increase the number and mass loading of atmospheric
424 organic particles, and release pollen associated allergens as respirable particles.(119) From the
425 perspective of climate, these fragmented particles can act as cloud condensation nuclei(120)
426 and ice nuclei.(121) From the health perspective, they may have an adverse impact on air
427 quality.

428 Fungal spores are smaller (1-6 μm in diameter) than pollen grains (5-150 μm), and have a
429 higher concentration (number: $\sim 10^4 \text{ m}^{-3}$; mass: $1 \mu\text{g m}^{-3}$) in the continental boundary
430 layer.(122) In tropical areas, such as the Amazon basin, fungal spores are a major fraction of
431 supermicron aerosol particles.(105) Recent studies show that, similar to pollens, fungal spores
432 can rupture when exposed to high relative humidity and subsequent drying. Figure 5 shows
433 selected SEM images of ruptured fungal spores after humidification and drying. Because new
434 particle formation events and subsequent growth of ultrafine particles are seldom observed in
435 the Amazon basin, their formation mechanisms remain enigmatic.(123) However, during the
436 wet season, bursting events of ultrafine particles in the diameter range of 10-40 nm are
437 frequent.(123) Expulsion of the nanoparticles and submicron particles from fungal spores under
438 moist conditions in the Amazon basin (relative humidity >70%) and/or outflow from deep
439 convective clouds (in-cloud processing of fungal spores) could be common in other tropical
440 areas and may provide insight into new particle formation. Chemical imaging and microscopy
441 characterization of substrate deposited particles and monitoring their transformations using
442 environmental cells are among the most promising methods to study spore fragmentation
443 phenomena and their climatic impacts.

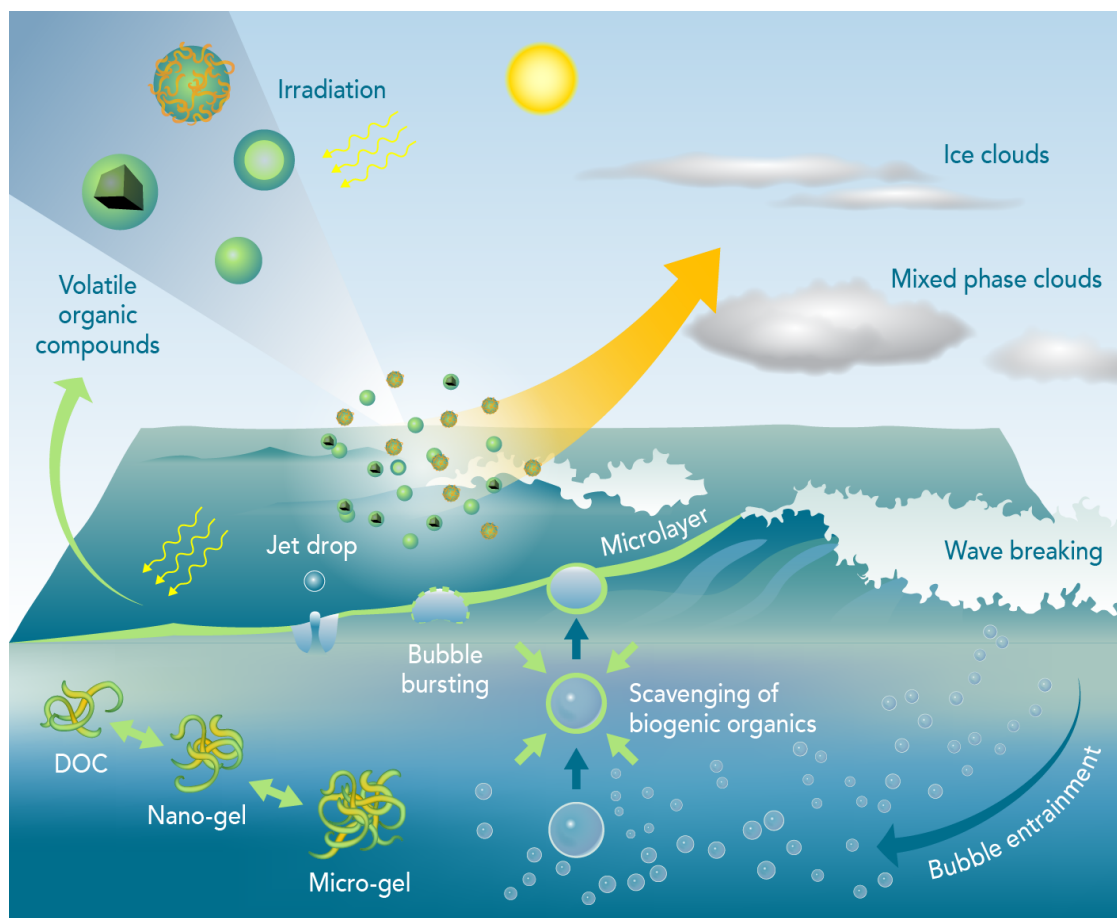
444



445
446 **Figure 5.** SEM images of fragmented fungal spores and expulsion of subfungal spore particles. The
447 examples shown in the images are fungal spores collected in the Amazonia. Images revealed that size of
448 the expelled fungal spores vary substantially, ranging from a few to hundreds nanometers. Scale bar is 2
449 μm .

450 3.3. Sea Spray Aerosol

451 The oceans cover about 71% of Earth surface and represent a continuous source of SSA,
452 emitted through wave breaking and bubble bursting. Figure 6 illustrates how SSA impacts cloud
453 formation, precipitation, atmospheric chemistry, and global climate.(91; 124) Recent studies,
454 supported by laboratory mesocosm experiments(125-128), have demonstrated transport of
455 organic material from the ocean to the atmosphere by SSA.(129-133) SSA particles show a
456 strong enhancement of the organic fraction with decreasing aerosol size.(27; 125; 128; 133)
457 Understanding SSA chemical composition is critical for predicting CCN activation and assessing
458 their effects on cloud formation and climate.(134; 135) Due to their chemical complexity and
459 variability in their external and internal mixing states, CCN activity of SSA is poorly
460 constrained.(127; 136; 137) Recent applications of chemical imaging techniques combined with
461 in-situ measurements revealed additional compositional details of SSA. Particles consisting of
462 only organic carbon species dominate sizes smaller than 180 nm and their number
463 concentration increases with increasing biological activity,(138) whereas SSA particles of larger
464 sizes typically contain sea salt cores coated with organic material.(27) The presence of bacteria
465 and phytoplankton in seawater affect the surfactant structure of large SSA, but have minor
466 impact on smaller (~ 150 nm) particles.(139) SSA particles generated during bacteria
467 metabolism indicate the presence of transition metals, likely due to bacterial
468 bioaccumulation or colloids adhering to these metal ions.(140)



470

471 **Figure 6.** Schematic diagram showing the complex interactions between subsurface water and sea
 472 surface microlayer, generation and composition of SSA particles, and implications for their atmospheric
 473 chemical and physical processes of the environmental and climate forcing relevance.(5; 91; 95)

474

475 Colloids and aggregates exuded by phytoplankton contribute to water insoluble organic
 476 matter of SSA.(133) Such gel-like particles are composed of tangled macromolecules and
 477 colloids, preferentially from surface-active polysaccharides(141) and proteinaceous
 478 materials.(142) These marine nano- and micro-gels are ubiquitous at the ocean surface, and
 479 therefore, contribute to the SSA composition. Marine gels have been detected in cloud water
 480 which suggests they have a significant role in CCN activation.(131) However, chemical
 481 characterization of gels within individual SSA particles, and their molecular-level variability, are
 482 mostly unknown. Physicochemical properties such as phase state, optical properties, and
 483 responses to hydration, dehydration, and temperature changes are also poorly understood.

484 As inferred from field studies, laboratory experiments, and atmospheric models, specific
 485 types of SSA particles significantly affect atmospheric ice nucleation.(95; 143; 144) A recent
 486 study,(95) demonstrated enhanced ice nucleation activity in SSML water samples collected in

487 the Atlantic and Pacific oceans under typical cloud conditions. Specifically, it was shown that
488 the ice nucleating components of SSA particles are < 200 nm in size and likely stem from
489 phytoplankton exudates. Chemical imaging of individual particles nucleating ice suggests that
490 aged marine particles can contribute to atmospheric ice crystal formation.(56) Wave channel
491 generated SSA particles exhibited ice formation potential when the total organic content in
492 seawater was similar to typical ocean background conditions.(128) All of these studies suggest
493 that biogenic material ejected from oceans as SSA components can impact atmospheric ice
494 nucleation. In addition to marine organisms such as viruses, marine gels may be potential IN
495 candidates.(145) However, none of the compounds directly responsible for ice nucleation has
496 been identified with a sufficient level of chemical specificity.

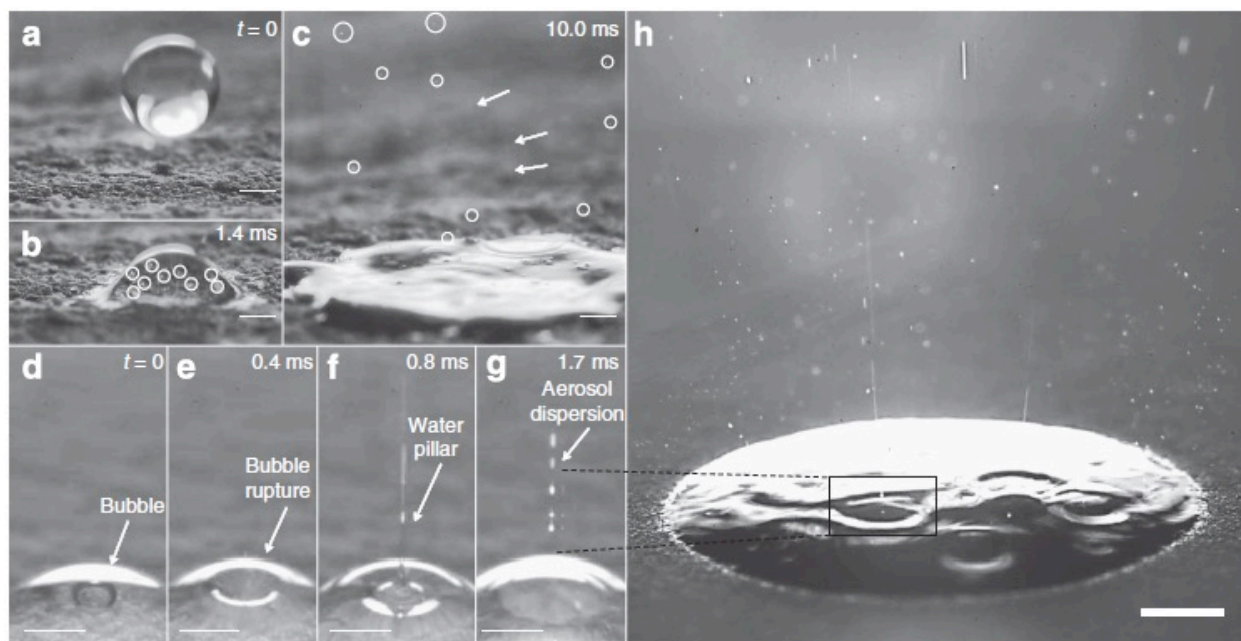
497 The composition of SSA particles defines their reactivity and transformations through
498 heterogeneous and multiphase atmospheric chemistry involving gas- and aqueous phase
499 oxidants. Photochemically induced reactions in the SSML change the nature of the organic
500 molecules available for ejection.(92; 146) Furthermore, photochemical reactions occurring in
501 SSA, lead to changes in the physicochemical properties of particles and in the gas-particle
502 partitioning of the products.(147) The mixing state and amount of organic material distributed
503 among different SSA particles may impact the underlying multiphase reaction mechanisms and
504 their kinetics. For example, laboratory studies of SSA reacting with HNO₃ demonstrated that
505 particle reactivity was correlated with the crystalline structure of the salt core and the amount
506 of organic carbon.(41) Reactive uptake by HNO₃ resulted in a redistribution of inorganic cations
507 and a layer of organic matter concentrated at the surface of the particle suggest that specific
508 ion and pH effects impact the physicochemical structures of SSA particles.(42) Atmospheric
509 aging and transformation of SSA through reactions with other common oxidants such as O₃ and
510 OH are not sufficiently known. The origin and composition of the organic matter in SSA is
511 substantially different from biogenic and anthropogenic OA. Hence, understanding atmospheric
512 chemistry and transformations of OA in the marine environment requires additional studies.

513

514 **3.4. Airborne Soil Organic Particles**

515 Until recently, it was believed that the primary processes for aerosolizing soils and
516 entraining their SOM constituents into the Earth's atmosphere were natural wind erosion and
517 human mechanical activities such as agricultural tilling or harvesting. However, recent field
518 observations provided evidence of a previously unrecognized mechanism of atmosphere – land
519 surface interactions that result in ejection of submicron ASOP after intensive precipitation
520 events such as rainfall or irrigation.(96) These observations were corroborated by a separately
521 reported laboratory study(148) showing that droplets impinging on wet mineral surfaces
522 generated fine aqueous mist. Figure 7 displays images, captured by a high-speed camera,
523 showing raindrop induced frenetic generation of bubbles within a layer of the surface
524 accumulated water followed by ejection of very fine aqueous particles upon bubble bursting.

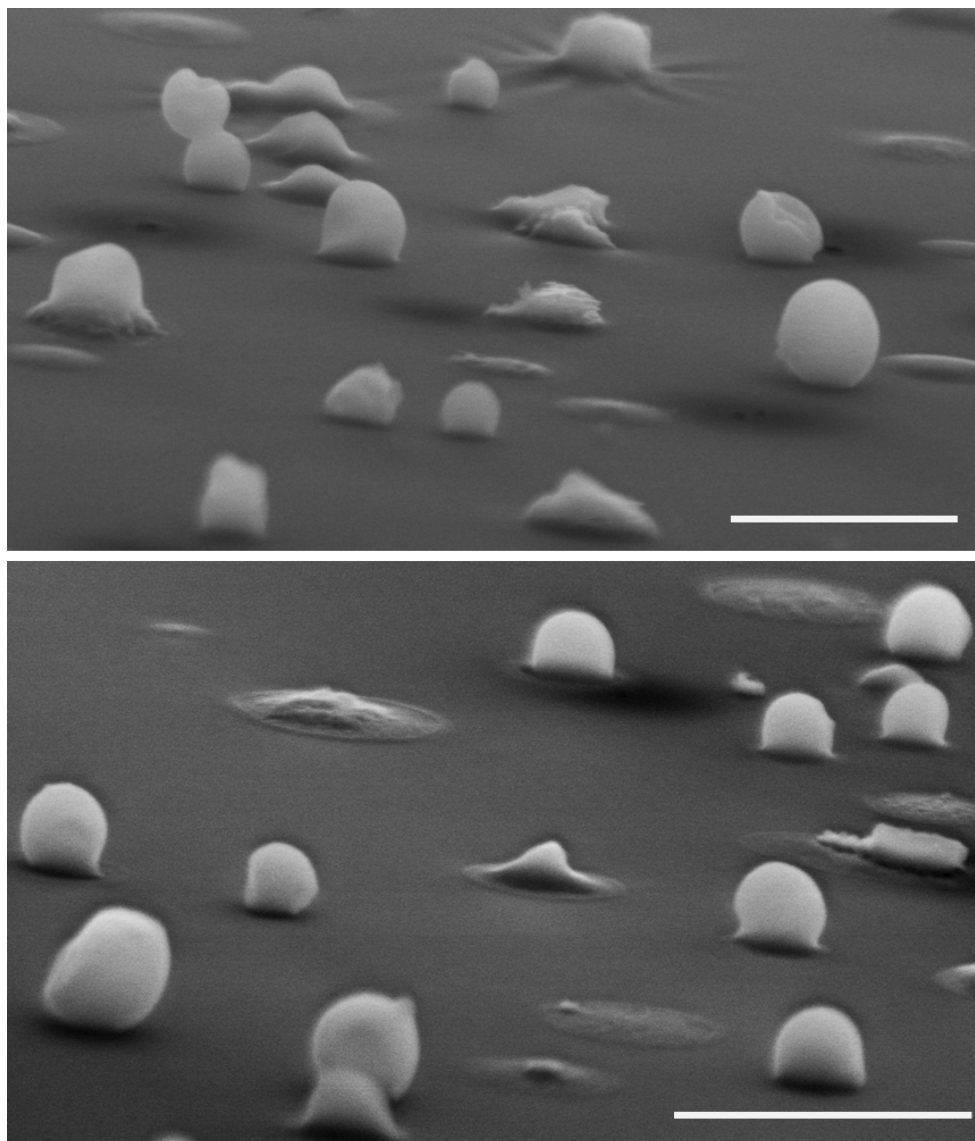
525 Similar to generation of organic sea spray particles, discussed in section 3.3., dissolved organic
526 matter from wet soils is aerosolized by bursting of entrained bubbles at the air-water interface.
527



528
529 **Figure 7.** High-speed images capturing the “raindrop mechanism” of aerosol generation. (a-c)
530 Impingement of a droplet onto solid mineral surface and formation of air bubbles inside of the aqueous
531 layer formed on the surface. (d-e) Dynamic ejection of a fine aqueous mist upon bursting of the air
532 bubbles at the air-water interface. (Reproduced with permission from reference (148). Copyright 2015
533 Nature Publishing Group).

534 Micro-spectroscopic chemical imaging and microanalysis of ASOP collected in a field study
535 in Oklahoma indicate that they appear as unusual spherical glassy organic solids, and their
536 characteristic X-ray absorption spectra match those of dissolved soil organic matter. Figure 8
537 illustrates their visual appearance in the SEM images taken at tilted angle.(96) The soil-derived
538 source and mechanism of ASOP formation were inferred based on the notable similarity of their
539 NEXAFS spectra to that of SOM. Typical molecular constituents of SOM are substantially larger
540 than common atmospheric organics. Therefore, evaporation of water from SOM-containing
541 aqueous mist results in solidification of resulting ASOP at ambient conditions, as confirmed by
542 the observed glassy-like spherical morphology. This additional, previously unrecognized type of
543 OA may have significant impacts on the atmospheric environment in areas where soils are
544 exposed to strong, episodic precipitation events such as agricultural systems or natural
545 grasslands.

546
547



548
549

550 **Figure 8.** SEM images at 75° tilt angle of solid ASOP sampled by the impaction method. High vertical
551 dimension of ASOP is indicative of their solid (glassy) phase.(96)

552

553 Inherent with their soil-derived composition and substantial content of carbon with sp^2
554 hybridization (C=C double bonds), ASOP may contribute substantially to atmospheric brown
555 carbon and its associated light absorption and scattering. ASOP advected aloft may ultimately
556 impact cloud properties and subsequent precipitation. Dynamic ESEM imaging of hydrating
557 ASOP confirmed that they remain water-soluble and CCN-active.(96) Furthermore, because of
558 their glassy phase, ASOP would provide solid surfaces for heterogeneous ice nucleation in cold
559 and mixed-phase clouds. Interestingly, the importance of SOM as strong IN has been
560 highlighted in numerous field and laboratory studies.(149-151) However, previously, airborne

561 SOM has always been attributed to the wind-blown erosion of soil, whereas direct emissions in
562 a form of ASOP were never considered.

563 Understanding sources and the chemical composition of solid organic particles lies at the
564 research forefront for the atmospheric chemistry community because of their unique
565 physicochemical properties that are directly relevant to climate change and public health. The
566 phase state of atmospheric organic particles plays a key role in their physicochemical
567 properties, interactions with water vapor, gas-particle partitioning, and reactivity, and thus, has
568 important implications in various environmental processes.(40; 152-156) Currently, research
569 efforts on the phase of OA are concentrated on atmospheric processes that solidify liquid-like
570 secondary organic particles produced through multi-phase atmospheric chemistry.(13; 157;
571 158) The concept of direct emissions of solid ASOP is not even considered.

572 Additionally, ASOP may impact the atmospheric environment as a carrier to transport
573 water-soluble nitrites from soils to airborne aqueous particles, where nitrite can be protonated
574 to form HONO and partition into the gas-phase. HONO is an important source of hydroxyl (OH)
575 radicals that control the oxidative capacity of the atmosphere. Release of HONO from soil
576 nitrites may substantially influence HONO and OH production in the atmosphere, and impact
577 the biogeochemical nitrogen cycle.(159; 160) The large surface area of ASOP may drastically
578 accelerate gas-phase release of HONO, and consequently affect processes influencing the
579 oxidative atmospheric environment.

580 Future studies should assess the relationship between rainfall intensity and efficiency of the
581 ASOP generation, evaluate and constrain ASOP budgets specific to different geographic regions,
582 describe region-specific variability in ASOP composition, understand their atmospheric
583 transformations, and quantify their optical and cloud nucleation properties.

584 Notably, ASOP are refractory and do not volatilize substantially upon heating up to 600
585 °C.(96) Hence, they would not be detected by common methods of in-situ particle speciation
586 based on thermal evaporation. Methods of laser ablation MS can certainly detect ASOP;
587 however, extensive fragmentation upon ablation could generate mass spectra that would be
588 confused with other organic particles. The solid (glassy) phase, and refractory carbonaceous
589 composition of ASOP make spectro-microscopy methods the most effective detection
590 techniques, and for assessing optical and hygroscopic properties. The structures of the high-
591 molecular weight constituents of ASOP are of particular interest because they control their
592 chemical and physical properties. Size-selected sampling of ASOP during events of their high
593 abundance, followed by advanced analysis using nano-DESI/HRMS can be utilized for probing
594 the molecular-level speciation of ASOP and ultimately for understanding their atmospheric
595 transformations.

596

597 **4. Summary**

598 Multi-modal applications of novel analytical platforms highlighted in this manuscript
599 facilitated in-depth chemical analysis of complex atmospheric particles. Methods of chemical
600 imaging and molecular-level analysis described herein provide experimental means to improve
601 fundamental knowledge of particle effects on cloud microphysics, their dependence on
602 variables (relative humidity, temperature, multi-phase reactions), and distinguishing chemistry
603 of natural and anthropogenic particles. The complex issues of aerosol chemistry and physics
604 utilize a consortium of expertise, methods and measurements that require a collaborative
605 framework and shared resources to provide coordinated, comprehensive, and multidisciplinary
606 approaches to advance our fundamental understanding of aerosol impact on climate change,
607 air quality, visibility and health issues. In recent years, we observed tremendous expansion and
608 growth of research in this area; a trend that likely will continue.

609 We highlighted several scientific challenges related to complex, multi-phase chemistry
610 and physics of atmospheric particles that could uniquely benefit from multi-modal
611 experimental approaches of chemical imaging and molecular-level analysis. The atmospheric
612 processes associated with these particles and their impacts on environment and climate remain
613 insufficiently understood, even at the phenomenological level, largely due to incomplete
614 information on the fundamental physicochemical properties of particles. These selected
615 examples highlight exciting opportunities in the field of aerosol environmental chemistry,
616 where multi-modal characterization of particles would significantly impact our fundamental
617 understanding of various air- surface interactions, and their influence on climate and air quality.

618 **5. Disclosure Statement**

619 The authors are not aware of any issues that might be perceived as affecting the
620 objectivity of this review.

621 **6. Acknowledgements**

622 The PNNL group acknowledges support from the Chemical Imaging Initiative of the Laboratory
623 Directed Research and Development program at Pacific Northwest National Laboratory (PNNL)
624 at the time of the manuscript's compilation. M.K.G. acknowledges support from the U.S.
625 Department of Energy's Atmospheric System Research, an Office of Science, Office of Biological
626 and Environmental Research program (DOE BER ASR). D.A.K. acknowledges support from DOE
627 BER ASR, U.S. National Science Foundation grants AGS-1232203 and AGS-1446286. Additional
628 support for previous and ongoing research projects in the authors' groups described in this
629 review has been provided by DOE BER through its sponsorship of the William R. Wiley
630 Environmental Molecular Sciences Laboratory (EMSL); the U.S. Department of Commerce,
631 National Oceanic and Atmospheric Administration through the Climate Program Office's AC4
632 program, award NA13OAR4310066 (A.L.); the Advanced Light Source by the Office of Basic
633 Energy Sciences, U.S. Department of Energy under Contract No. DE-AC02-05CH11231; beamline

634 11.0.2 is supported by Division of Chemical Sciences, Geosciences, and Biosciences and
635 Condensed Phase and Interfacial Molecular Sciences Program.
636

637 **Acronyms and Definitions**

638 **Aerosol:** mixture of airborne particles and gases at dynamic equilibrium.
639 (typeset next to the text lines 47-50)

640 **Radiative forcing of climate:** difference in the amount of sunlight energy absorbed by the Earth
641 and energy radiated back to space
642 (typeset next to the text lines 55-56)

643 **SEM:** scanning electron microscope; CCSEM – computer controlled SEM, ESEM – environmental
644 SEM, FIB/SEM – Focused ion beam system interfaced with SEM
645 (typeset next to the text lines 105-106)

646 **EDX:** Energy dispersed analyzer of X-rays
647 (typeset next to the text lines 105-106)

648 **HRTEM:** High resolution transmission electron microscope
649 (typeset next to the text lines 105-106)

650 **EELS:** Electron energy loss spectroscopy
651 (typeset next to the text lines 105-106)

652 **STXM/NEXAFS:** Scanning transmission x-ray microscope with near edges X-ray absorption fine
653 structure spectroscopy
654 (typeset next to the text lines 105-106)

655 **TOF-SIMS:** Time-of-flight secondary ionization mass spectrometer
656 (typeset next to the text lines 105-106)

657 **nano-SIMS:** SIMS instrument with magnetic sector mass analyzer optimized for ion probe
658 imaging with high lateral resolution and accurate isotopic measurements.
659 (typeset next to the text lines 105-106)

660 **Micro-Raman and Micro-FTIR:** Raman and Fourier transform infrared spectrometers interfaced
661 with optical microscopes for analysis of confined micrometer-size sample areas.
662 (typeset next to the text lines 105-106)

663 **CCN and IN:** cloud condensation nuclei and ice nuclei
664 (typeset next to the text line 172)

665 **RH:** relative humidity
666 (typeset next to the text line 243)

667 **OA:** organic aerosol
668 (typeset next to the text line 263)

669 **HRMS:** high resolution mass spectrometry
670 (typeset next to the text line 265)

671 **Nano-DESI:** nanospray electrospray ionization
672 (typeset next to the text line 267)

673 **SSA:** sea spray aerosol
674 (typeset next to the text line 451)

675 **SSML:** sea surface microlayer
676 (typeset next to the text line 486)

677 **SOM:** soil organic matter
678 (typeset next to the text line 516)

679 **ASOP:** airborne soil organic particles
680 (typeset next to the text line 519)

681

682

683 **Side Bars**

684 REACTIVITY OF INORGANIC PARTICLES WITH WEAK ORGANIC ACIDS
685 (typeset next to section 2.2)

686 Unique atmospheric reactions of aerosolized particles were inferred from chemical imaging of
687 individual marine particles.(26) Chloride, carbonate, and nitrate components of inorganic
688 particles (e.g. sea salt and selected components of mineral dust) may react with water soluble
689 organic acids releasing volatile gas-phase products (HCl, CO₂, HNO₃) to the atmosphere, leaving
690 behind particles enriched in the organic salts. While these reactions are not thermodynamically
691 favored for bulk aqueous chemistry, these reactions in aerosol are driven by evaporation of the
692 volatile products from drying particles. Field observations(26) of these particle transformations
693 were corroborated in a number of laboratory experiments(39; 40) indicating that substantial
694 reactivity between inorganic and organics components within aged particles and its potential
695 impact on the modification of hygroscopic and optical properties of aerosols.

696

697 MOLECULAR IDENTITY OF ORGANIC AEROSOLS
698 (typeset next to section 2.3)

699 Recent advances in molecular-level characterization of OA facilitate new opportunities for
700 improved understanding of its formation mechanisms, source apportionment and atmospheric
701 transformations. Here, we highlight several new studies where deciphering molecular identity
702 of OA identifies perspective areas for future research. Specifically, the molecular-level HRMS
703 data can be used as a fingerprint for advanced source apportionment of ambient OA based on
704 the comparative analysis with its laboratory mimics,(87) or by identifying molecular markers of
705 the source specific precursors.(93) Multiple reports suggest that selected OA components may
706 have a distinct effect on its overall “brown carbon” properties evoking additional studies
707 focused on the molecular characterization of light-absorbing components within complex matrix
708 of OA.(22) Explicit description of OA molecular components can be used for model
709 estimates(161) of particle viscosity and phase state providing critical insights into
710 transformation of OA physicochemical properties and atmospheric life cycle.

711

712 SURFACE-MEDIATED REACTIOS OF DUST PROMOTE NEW PARTICLE FORMATION
713 (typeset next to section 3.1)

714 Field observations at a mountain site in South China reported an unexpected impact of mineral
715 dust on new particle formation and growth.(97) Enhanced events of new particle formation and

716 growth were systematically observed during high-loading episodes of mineral dust aged by
717 anthropogenic pollution. These observations were ascribed to plausible dust induced multi-
718 facet photochemistry, where photolytic decomposition of complex organic compounds
719 releasing volatile nucleating products was suggested. These findings challenge the traditional
720 wisdom that mineral dust acts mostly as a sink for atmospheric oxidants, and suggested that
721 when mineral dust and pollution are mixed they may have photocatalytic feedback that
722 provides an unrecognized source of OH radical and other oxidants.

723

724 NEW PARTICLES FROM FRAGMENTATION OF BIOLOGICAL SPORES 725 (typeset next to section 3.2)

726 Observations from our ongoing experiments show that fungal spores can rupture when
727 exposed to high relative humidity (~98% RH) and subsequent drying. In this study, we are
728 investigating biological particles collected during the wet season in 2015 at a pristine rainforest
729 site in Central Amazonia. Figure 5 shows an example of fragmented and expelled fungal spores
730 after wet and drying cycles. The rupture process expels tens to hundreds of fine subfungal
731 particles ranging from a few to hundreds of nanometers in size. In particular, a substantial
732 variation in number, size, and composition was observed for fragmented particles from the
733 ruptured fungal spores.

734

735 ICE-NUCLEATING PROPENSITY OF ORGANIC PARTICLES 736 (typeset next to section 3.3)

737 Ice nucleation experiments using a controlled vapor cooling-stage microscope system and
738 complemented by chemical imaging(56; 95; 143) indicate substantial presence of organics in
739 ice-nucleating particles. Experiments with SSA particles collected at different locations above
740 the ocean surf zone, laboratory mesocosm experiments, and Atlantic ocean show that particles
741 larger than 300 nm in diameter initiate ice nucleation under conditions relevant to mixed-phase
742 and cirrus clouds. Identified ice-nucleating particles contain inorganic cores of sea salt
743 surrounded by organic outer layers. Chemical imaging reveals alcohol and carboxyl
744 functionalities in the organic material and suggests that the organic coating is highly viscous.
745 These observations support the potential for organic particles to affect ice nucleation in the
746 atmosphere.

747

748 RAINFALL GENERATES SOLID ORGANIC PARTICLES

749 (typeset next to section 3.4)

750

751 Solidified ASOP – airborne soil organic particles can be generated as a result of atmosphere –
752 land surface interactions through a recently revealed “raindrop mechanism”(148) when water
753 droplets, during precipitation or irrigation events, hit open soil surfaces.(96) Field observations
754 showed a dominant presence of solid ASOP (60% by number) after an intensive rain event at
755 Southern Great Plains, Oklahoma, USA – an agricultural region where large areas of cultivated
756 land are exposed to ambient air. Physicochemical properties of ASOP, investigated by chemical
757 imaging and microanalysis techniques, suggest that they may serve as cloud condensation and
758 ice nuclei, absorb solar radiation, and impact the atmospheric environment and carbon cycle at
759 local and regional scales.

760

761

762

763

764

765 7. Literature Cited

766 Annotated references:

- 767 **Ref 1** An excellent review of aerosol chemistry highlighting synergism between laboratory studies,
768 field measurements and modeling analysis.
- 769 **Ref 5.** Comprehensive review of aerosol multiphase chemistry influencing the Earth system, climate,
770 air quality, and public health.
- 771 **Ref 16.** A review manuscript featuring applications and perspectives of the HRMS analysis for
772 molecular-level studies of organic aerosols.
- 773 **Ref 17.** An edited book offering the comprehensive overview of the spectroscopy of aerosols,
774 including fundamental aspects and applications.
- 775 **Ref 22.** Thorough review focused on the current understanding of the chemistry of atmospheric
776 brown carbon, including highlights of areas that need further studies.
- 777 **Ref 91.** A comprehensive review of the results of field and laboratory studies performed to
778 characterize the properties of SSA, with an emphasis on the organic fraction.
- 779 **Ref 92.** A comprehensive review of photochemical processes occurring at the air-surface interfaces of
780 aerosols, environmental surfaces and atmospheric ice.
- 781 **Ref 96.** The field evidence report of solid ASOP emitted to the atmosphere through atmosphere – land
782 surface interactions following rainfall.
- 783 **Ref 98.** An edited book offering the comprehensive overview of the chemistry and physics of
784 atmospheric mineral dust.
- 785 **Refs 106,107.** Comprehensive reviews focused on the airborne biological particles, theirs atmospheric
786 lifecycles and impacts on air quality and climate.
- 787
- 788 1. Prather KA, Hatch CD, Grassian VH. 2008. Analysis of Atmospheric Aerosols. In *Annual Review of*
789 *Analytical Chemistry*, 1:485-514. Number of 485-514 pp.
- 790 2. Boucher O, Randall D, Artaxo P, Bretherton C, Feingold G, et al. 2013. Clouds and Aerosols. In
791 *Climate Change 2013: The Physical Science Basis. Contribution of Working Group I to the Fifth*
792 *Assessment Report of the Intergovernmental Panel on Climate Change*, ed. TF Stocker, D Qin, G-
793 K Plattner, M Tignor, SK Allen, et al:571-658. Cambridge, United Kingdom and New York, NY,
794 USA.: Cambridge University Press, . Number of 571-658 pp.
- 795 3. von Schneidemesser E, Monks PS, Allan JD, Bruhwiler L, Forster P, et al. 2015. Chemistry and the
796 Linkages between Air Quality and Climate Change. *Chem. Rev.* 115:3856-97

- 797 4. Moosmueller H, Chakrabarty RK, Arnott WP. 2009. Aerosol light absorption and its
798 measurement: A review. *J. Quant. Spectr. Rad. Transfer* 110:844-78
- 799 5. Poeschl U, Shiraiwa M. 2015. Multiphase Chemistry at the Atmosphere-Biosphere Interface
800 Influencing Climate and Public Health in the Anthropocene. *Chem. Rev.* 115:4440-75
- 801 6. Fowler D, Pilegaard K, Sutton MA, Ambus P, Raivonen M, et al. 2009. Atmospheric composition
802 change: Ecosystems-Atmosphere interactions. *Atmos. Environ.* 43:5193-267
- 803 7. Ridgwell AJ. 2002. Dust in the Earth system: the biogeochemical linking of land, air and sea.
804 *Philosophical Transactions of the Royal Society of London Series a-Mathematical Physical and*
805 *Engineering Sciences* 360:2905-24
- 806 8. Pratt KA, Prather KA. 2012. Mass spectrometry of atmospheric aerosols. Recent developments
807 and applications. Part I: Off-line mass spectrometry techniques. *Mass Spectrom. Rev.* 31:1-16
- 808 9. Pratt KA, Prather KA. 2012. Mass spectrometry of atmospheric aerosols. Recent developments
809 and applications. Part II: On-line mass spectrometry techniques. *Mass Spectrom. Rev.* 31:17-48
- 810 10. Laskin A, Laskin J, Nizkorodov SA. 2012. Mass spectrometric approaches for chemical
811 characterisation of atmospheric aerosols: critical review of the most recent advances. *Environ.*
812 *Chem.* 9:163-89
- 813 11. Laskin J, Laskin A, Nizkorodov SA. 2013. New Mass Spectrometry Techniques for Studying
814 Physical Chemistry of Particles, Droplets, and Surfaces. *International Reviews in Physical*
815 *Chemistry* 32:128-70
- 816 12. Canagaratna MR, Jayne JT, Jimenez JL, Allan JD, Alfarra MR, et al. 2007. Chemical and
817 microphysical characterization of ambient aerosols with the aerodyne aerosol mass
818 spectrometer. *Mass Spectrom. Rev.* 26:185-222
- 819 13. Krieger UK, Marcolli C, Reid JP. 2012. Exploring the complexity of aerosol particle properties and
820 processes using single particle techniques. *Chem. Soc. Rev.* 41:6631-62
- 821 14. Bzdek BR, Pennington MR, Johnston MV. 2012. Single particle chemical analysis of ambient
822 ultrafine aerosol: A review. *J. Aerosol Sci* 52:109-20
- 823 15. Duarte R, Duarte AC. 2011. A critical review of advanced analytical techniques for water-soluble
824 organic matter from atmospheric aerosols. *Trac-Trends in Anal. Chem.* 30:1659-71
- 825 16. Nizkorodov SA, Laskin J, Laskin A. 2011. Molecular chemistry of organic aerosols through the
826 application of high resolution mass spectrometry. *PCCP* 13:3612-29
- 827 17. Signorell R, Reid JP, eds. 2011. *Fundamentals and Applications in Aerosol Spectroscopy*. Boca
828 Raton London New York: CRC Press, Taylor & Francis Group. 509 pp.
- 829 18. Kulkarni P, Baron PA, Willeke K, eds. 2011. *Aerosol measurement: Principles, Techniques, and*
830 *Applications*. Hoboken, NJ: John Wiley & Sons, Inc. 884 pp.
- 831 19. Posfai M, Buseck PR. 2010. Nature and Climate Effects of Individual Tropospheric Aerosol
832 Particles. In *Annual Review of Earth and Planetary Sciences, Vol 38*, ed. R Jeanloz, KH Freeman,
833 38:17-43. Number of 17-43 pp.
- 834 20. Moffet RC, Tivanski AV, Gilles MK. 2010. Scanning X-ray Transmission Microscopy: Applications
835 in Atmospheric Aerosol Research. In *Fundamentals and Applications in Aerosol Spectroscopy*, ed.
836 R Signorell, JP Reid:419-62: Taylor and Francis Books, Inc. Number of 419-62 pp.
- 837 21. Laskin A. 2010. Electron Beam Analysis and Microscopy of Individual Particles. In *Fundamentals*
838 *and Applications in Aerosol Spectroscopy*, ed. R Signorell, JP Reid:463-91: Taylor and Francis
839 Books, Inc. Number of 463-91 pp.
- 840 22. Laskin A, Laskin J, Nizkorodov SA. 2015. Chemistry of Atmospheric Brown Carbon. *Chem. Rev.*
841 115:4335-82
- 842 23. Moffet RC, Roedel TC, Kelly ST, Yu XY, Carroll GT, et al. 2013. Spectro-microscopic
843 measurements of carbonaceous aerosol aging in Central California. *Atmos. Chem. Phys.*
844 13:10445-59

- 845 24. O'Brien RE, Wang B, Laskin A, Riemer N, West M, et al. 2015. Chemical imaging of ambient
846 aerosol particles: Observational constraints on mixing state parameterization. *J. Geophys. Res. -*
847 *Atmos.* 120:9591–605
- 848 25. Hiranuma N, Brooks SD, Moffet RC, Glen A, Laskin A, et al. 2013. Chemical characterization of
849 individual particles and residuals of cloud droplets and ice crystals collected on board research
850 aircraft in the ISDAC 2008 study. *J. Geophys. Res. - Atmos.* 118:6564-79
- 851 26. Laskin A, Moffet RC, Gilles MK, Fast JD, Zaveri RA, et al. 2012. Tropospheric chemistry of
852 internally mixed sea salt and organic particles: Surprising reactivity of NaCl with weak organic
853 acids. *J. Geophys. Res. - Atmos.* 117:D15302, 10.1029/2012jd017743
- 854 27. Ault AP, Moffet RC, Baltrusaitis J, Collins DB, Ruppel MJ, et al. 2013. Size-Dependent Changes in
855 Sea Spray Aerosol Composition and Properties with Different Seawater Conditions. *Environ. Sci.*
856 *Techol.* 47:5603-12
- 857 28. Conny JM, Collins SM, Herzing AA. 2014. Qualitative Multiplatform Microanalysis of Individual
858 Heterogeneous Atmospheric Particles from High-Volume Air Samples. *Anal. Chem.* 86:9709-16
- 859 29. Kim Y-H, Kim K-H, Ma C-J, Shon Z-H, Park CG, et al. 2014. An investigation into the relationship
860 between the major chemical components of particulate matter in urban air. *Chemosphere*
861 95:387-94
- 862 30. Jung H-J, Eom H-J, Kang H-W, Moreau M, Sobanska S, Ro C-U. 2014. Combined use of
863 quantitative ED-EPMA, Raman microspectrometry, and ATR-FTIR imaging techniques for the
864 analysis of individual particles. *Analyst* 139:3949-60
- 865 31. Jeong GY, Achterberg EP. 2014. Chemistry and mineralogy of clay minerals in Asian and Saharan
866 dusts and the implications for iron supply to the oceans. *Atmos. Chem. Phys.* 14:12415-28
- 867 32. Eom H-J, Jung H-J, Sobanska S, Chung S-G, Son Y-S, et al. 2013. Iron Speciation of Airborne
868 Subway Particles by the Combined Use of Energy Dispersive Electron Probe X-ray Microanalysis
869 and Raman Microspectrometry. *Anal. Chem.* 85:10424-31
- 870 33. Jeong GY, Kim JY, Seo J, Kim GM, Jin HC, Chun Y. 2014. Long-range transport of giant particles in
871 Asian dust identified by physical, mineralogical, and meteorological analysis. *Atmos. Chem. Phys.*
872 14:505-21
- 873 34. Pohlker C, Huffman JA, Forster JD, Poschl U. 2013. Autofluorescence of atmospheric bioaerosols:
874 spectral fingerprints and taxonomic trends of pollen. *Atmospheric Measurement Techniques*
875 6:3369-92
- 876 35. Moffet RC, Furutani H, Rödel TC, Henn TR, Sprau PO, et al. 2012. Iron Speciation and Mixing in
877 Single Aerosol Particles from the Asian Continental Outflow. *Journal of Geophysical Research*
878 117:D07204, doi:10.1029/2011JD016746
- 879 36. Adachi K, Buseck PR. 2015. Changes in shape and composition of sea-salt particles upon aging in
880 an urban atmosphere. *Atmos. Environ.* 100:1-9
- 881 37. Adachi K, Zaizen Y, Kajino M, Igarashi Y. 2014. Mixing state of regionally transported soot
882 particles and the coating effect on their size and shape at a mountain site in Japan. *J. Geophys.*
883 *Res. - Atmos.* 119:5386-96
- 884 38. China S, Salvadori N, Mazzoleni C. 2014. Effect of Traffic and Driving Characteristics on
885 Morphology of Atmospheric Soot Particles at Freeway On-Ramps. *Environ. Sci. Techol.* 48:3128-
886 35
- 887 39. Wang B, Laskin A. 2014. Reactions between water-soluble organic acids and nitrates in
888 atmospheric aerosols: Recycling of nitric acid and formation of organic salts. *J. Geophys. Res. -*
889 *Atmos.* 119:3335-51
- 890 40. Wang BB, O'Brien RE, Kelly ST, Shilling JE, Moffet RC, et al. 2015. Reactivity of Liquid and
891 Semisolid Secondary Organic Carbon with Chloride and Nitrate in Atmospheric Aerosols. *J. Phys.*
892 *Chem. A* 119:4498-508

- 893 41. Ault AP, Guasco TL, Baltrusaitis J, Ryder OS, Trueblood JV, et al. 2014. Heterogeneous Reactivity
894 of Nitric Acid with Nascent Sea Spray Aerosol: Large Differences Observed between and within
895 Individual Particles. *J. Phys. Chem. Lett.* 5:2493-500
- 896 42. Ault AP, Guasco TL, Ryder OS, Baltrusaitis J, Cuadra-Rodriguez LA, et al. 2013. Inside versus
897 Outside: Ion Redistribution in Nitric Acid Reacted Sea Spray Aerosol Particles as Determined by
898 Single Particle Analysis. *J. Am. Chem. Soc.* 135:14528-31
- 899 43. Veghte DP, Altaf MB, Freedman MA. 2013. Size Dependence of the Structure of Organic Aerosol.
900 *J. Am. Chem. Soc.* 135:16046-9
- 901 44. Ghorai S, Wang B, Tivanski A, Laskin A. 2014. Hygroscopic Properties of Internally Mixed
902 Particles Composed of NaCl and Water-Soluble Organic Acids. *Environ. Sci. Technol.* 48:2234-41
- 903 45. Li X, Gupta D, Eom H-J, Kim H, Ro C-U. 2014. Deliquescence and efflorescence behavior of
904 individual NaCl and KCl mixture aerosol particles. *Atmos. Environ.* 82:36-43
- 905 46. Kim H, Lee M-J, Jung H-J, Eom H-J, Maskey S, et al. 2012. Hygroscopic behavior of wet dispersed
906 and dry deposited NaNO₃ particles. *Atmos. Environ.* 60:68-75
- 907 47. Mikhailov EF, Mironov GN, Poehlker C, Chi X, Krueger ML, et al. 2015. Chemical composition,
908 microstructure, and hygroscopic properties of aerosol particles at the Zotino Tall Tower
909 Observatory (ZOTTO), Siberia, during a summer campaign. *Atmos. Chem. Phys.* 15:8847-69
- 910 48. O'Brien RE, Wang BB, Kelly ST, Lundt N, You Y, et al. 2015. Liquid-Liquid Phase Separation in
911 Aerosol Particles: Imaging at the Nanometer Scale. *Environ. Sci. Technol.* 49:4995-5002
- 912 49. You Y, Renbaum-Wolff L, Carreras-Sospedra M, Hanna SJ, Hiranuma N, et al. 2012. Images reveal
913 that atmospheric particles can undergo liquid-liquid phase separations. *Proc. Natl. Acad. Sci.*
914 *U.S.A.* 109:13188-93
- 915 50. You Y, Renbaum-Wolff L, Bertram AK. 2013. Liquid-liquid phase separation in particles
916 containing organics mixed with ammonium sulfate, ammonium bisulfate, ammonium nitrate or
917 sodium chloride. *Atmos. Chem. Phys.* 13:11723-34
- 918 51. Pohlker C, Saturno J, Kruger ML, Forster JD, Weigand M, et al. 2014. Efflorescence upon
919 humidification? X-ray microspectroscopic in situ observation of changes in aerosol
920 microstructure and phase state upon hydration. *Geophys. Res. Lett.* 41:3681-9
- 921 52. Ghosal S, Weber PK, Laskin A. 2014. Spatially resolved chemical imaging of individual
922 atmospheric particles using nanoscale imaging mass spectrometry: insight into particle origin
923 and chemistry. *Analytical Methods* 6:2444-51
- 924 53. Chen HH, Grassian VH, Saraf LV, Laskin A. 2013. Chemical imaging analysis of environmental
925 particles using the focused ion beam/scanning electron microscopy technique: microanalysis
926 insights into atmospheric chemistry of fly ash. *Analyst* 138:451-60
- 927 54. Conny JM. 2013. Internal Composition of Atmospheric Dust Particles from Focused Ion-Beam
928 Scanning Electron Microscopy. *Environ. Sci. Technol.* 47:8575-81
- 929 55. Jeong GY, Nousiainen T. 2014. TEM analysis of the internal structures and mineralogy of Asian
930 dust particles and the implications for optical modeling. *Atmos. Chem. Phys.* 14:7233-54
- 931 56. Knopf DA, Alpert PA, Wang B, O'Brien RE, Kelly ST, et al. 2014. Microspectroscopic imaging and
932 characterization of individually identified ice nucleating particles from a case field study. *J.*
933 *Geophys. Res. - Atmos.* 119
- 934 57. Wang B, Laskin A, Roedel T, Gilles MK, Moffet RC, et al. 2012. Heterogeneous ice nucleation and
935 water uptake by field-collected atmospheric particles below 273 K. *J. Geophys. Res. - Atmos.* 117
- 936 58. Schill GP, Genareau K, Tolbert MA. 2015. Deposition and immersion-mode nucleation of ice by
937 three distinct samples of volcanic ash. *Atmos. Chem. Phys.* 15:7523-36
- 938 59. Sihvonen SK, Schill GP, Lykтей NA, Veghte DP, Tolbert MA, Freedman MA. 2014. Chemical and
939 Physical Transformations of Aluminosilicate Clay Minerals Due to Acid Treatment and
940 Consequences for Heterogeneous Ice Nucleation. *J. Phys. Chem. A* 118:8787-96

- 941 60. Schill GP, Tolbert MA. 2014. Heterogeneous Ice Nucleation on Simulated Sea-Spray Aerosol
942 Using Raman Microscopy. *Journal of Physical Chemistry C* 118:29234-41
- 943 61. Wheeler MJ, Mason RH, Steunenberg K, Wagstaff M, Chou C, Bertram AK. 2015. Immersion
944 Freezing of Supermicron Mineral Dust Particles: Freezing Results, Testing Different Schemes for
945 Describing Ice Nucleation, and Ice Nucleation Active Site Densities. *J. Phys. Chem. A* 119:4358-72
- 946 62. Thompson JE, Hayes PL, Jimenez JL, Adachi K, Zhang X, et al. 2012. Aerosol optical properties at
947 Pasadena, CA during CalNex 2010. *Atmos. Environ.* 55:190-200
- 948 63. Veghte DP, Freedman MA. 2012. The Necessity of Microscopy to Characterize the Optical
949 Properties of Size-Selected, Nonspherical Aerosol Particles. *Anal. Chem.* 84:9101-8
- 950 64. China S, Scarnato B, Owen RC, Zhang B, Ampadu MT, et al. 2015. Morphology and mixing state
951 of aged soot particles at a remote marine free troposphere site: Implications for optical
952 properties. *Geophys. Res. Lett.* 42:1243-50
- 953 65. Harris E, Sinha B, Hoppe P, Ono S. 2013. High-Precision Measurements of S-33 and S-34
954 Fractionation during SO₂ Oxidation Reveal Causes of Seasonality in SO₂ and Sulfate Isotopic
955 Composition. *Environ. Sci. Technol.* 47:12174-83
- 956 66. Harris E, Sinha B, van Pinxteren D, Schneider J, Poulain L, et al. 2014. In-cloud sulfate addition to
957 single particles resolved with sulfur isotope analysis during HCCT-2010. *Atmos. Chem. Phys.*
958 14:4219-35
- 959 67. Moffet RC, Henn TR, Laskin A, Gilles MK. 2010. Automated Chemical Analysis of Internally Mixed
960 Aerosol Particles Using X-ray Spectromicroscopy at the Carbon K-Edge. *Anal. Chem.* 82:7906-14
- 961 68. Kelly ST, Nigge P, Prakash S, Laskin A, Wang BB, et al. 2013. An environmental sample chamber
962 for reliable scanning transmission x-ray microscopy measurements under water vapor. *Rev. Sci.*
963 *Instrum.* 84
- 964 69. Huthwelker T, Zelenay V, Birrer M, Krepelova A, Raabe J, et al. 2010. An in situ cell to study
965 phase transitions in individual aerosol particles on a substrate using scanning transmission x-ray
966 microspectroscopy. *Rev. Sci. Instrum.* 81
- 967 70. Zelenay V, Ammann M, Krepelova A, Birrer M, Tzvetkov G, et al. 2011. Direct observation of
968 water uptake and release in individual submicrometer sized ammonium sulfate and ammonium
969 sulfate/adipic acid particles using X-ray microspectroscopy. *J. Aerosol Sci* 42:38-51
- 970 71. Benninghoven A. 1994. Chemical Analysis of Inorganic and Organic Surfaces and Thin Films by
971 Static Time-of-Flight Secondary Ion Mass Spectrometry (TOF-SIMS). *Angewandte Chemie*
972 *International Edition in English* 33:1023-43
- 973 72. Tervahattu H, Juhanaja J, Kupiainen K. 2002. Identification of an organic coating on marine
974 aerosol particles by TOF-SIMS. *J. Geophys. Res. - Atmos.* 107
- 975 73. Cheng W, Weng L-T, Li Y, Lau A, Chan C, Chan C-M. 2014. Characterization of size-segregated
976 aerosols using ToF-SIMS imaging and depth profiling. *Surf. Interface Anal.* 46:480-8
- 977 74. Liu Y, Minofar B, Desyaterik Y, Dames E, Zhu Z, et al. 2011. Internal structure, hygroscopic and
978 reactive properties of mixed sodium methanesulfonate-sodium chloride particles. *PCCP*
979 13:11846-57
- 980 75. Harris E, Sinha B, van Pinxteren D, Tilgner A, Fomba KW, et al. 2013. Enhanced Role of Transition
981 Metal Ion Catalysis During In-Cloud Oxidation of SO₂. *Science* 340:727-30
- 982 76. Laskina O, Young MA, Kleiber PD, Grassian VH. 2013. Infrared extinction spectroscopy and
983 micro-Raman spectroscopy of select components of mineral dust mixed with organic
984 compounds. *J. Geophys. Res. - Atmos.* 118:6593-606
- 985 77. Ault AP, Zhao D, Ebben CJ, Tauber MJ, Geiger FM, et al. 2013. Raman microspectroscopy and
986 vibrational sum frequency generation spectroscopy as probes of the bulk and surface
987 compositions of size-resolved sea spray aerosol particles. *PCCP* 15:6206-14

- 988 78. Craig RL, Bondy AL, Ault AP. 2015. Surface Enhanced Raman Spectroscopy Enables Observations
989 of Previously Undetectable Secondary Organic Aerosol Components at the Individual Particle
990 Level. *Anal. Chem.* 87:7510-4
- 991 79. Beardsley R, Jang M, Ori B, Im Y, Delcomyn CA, Witherspoon N. 2013. Role of sea salt aerosols in
992 the formation of aromatic secondary organic aerosol: yields and hygroscopic properties.
993 *Environ. Chem.* 10:167-77
- 994 80. Drozd G, Woo J, Hakkinen SAK, Nenes A, McNeill VF. 2014. Inorganic salts interact with oxalic
995 acid in submicron particles to form material with low hygroscopicity and volatility. *Atmos. Chem.*
996 *Phys.* 14:5205-15
- 997 81. Zaveri RA, Shaw WJ, Cziczo DJ, Schmid B, Ferrare RA, et al. 2012. Overview of the 2010
998 Carbonaceous Aerosols and Radiative Effects Study (CARES). *Atm. Chem. Phys. Diss.* 12:1299-400
- 999 82. Yancey Piens DS, Kelly ST, Harder TH, Petters MD, O'Brien RE, et al. 2015. Measuring Mass-
1000 Based Hygroscopicity of Atmospheric Particles through in situ Imaging. *Environ. Sci.*
1001 *Techol.*:submitted
- 1002 83. Roach PJ, Laskin J, Laskin A. 2010. Molecular Characterization of Organic Aerosols Using
1003 Nanospray-Desorption/Electrospray Ionization-Mass Spectrometry. *Anal. Chem.* 82:7979-86
- 1004 84. Laskin J, Laskin A, Roach PJ, Slysz GW, Anderson GA, et al. 2010. High-Resolution Desorption
1005 Electrospray Ionization Mass Spectrometry for Chemical Characterization of Organic Aerosols.
1006 *Anal. Chem.* 82:2048-58
- 1007 85. O'Brien RE, Laskin A, Laskin J, Rubitschun CL, Surratt JD, Goldstein AH. 2014. Molecular
1008 characterization of S- and N-containing organic constituents in ambient aerosols by negative ion
1009 mode high-resolution Nanospray Desorption Electrospray Ionization Mass Spectrometry: CalNex
1010 2010 field study. *J. Geophys. Res. - Atmos.* 119:12706-20
- 1011 86. O'Brien RE, Laskin A, Laskin J, Liu S, Weber R, et al. 2013. Molecular characterization of organic
1012 aerosol using nanospray desorption/electrospray ionization mass spectrometry: CalNex 2010
1013 field study. *Atmos. Environ.* 68:265-72
- 1014 87. O'Brien RE, Nguyen TB, Laskin A, Laskin J, Hayes PL, et al. 2013. Probing molecular associations
1015 of field-collected and laboratory-generated SOA with nano-DESI high-resolution mass
1016 spectrometry. *J. Geophys. Res. - Atmos.* 118:1042-51
- 1017 88. Tao S, Lu X, Levac N, Bateman AP, Nguyen TB, et al. 2014. Molecular Characterization of
1018 Organosulfates in Organic Aerosols from Shanghai and Los Angeles Urban Areas by Nanospray-
1019 Desorption Electrospray Ionization High-Resolution Mass Spectrometry. *Environ. Sci. Techol.*
1020 48:10993-1001
- 1021 89. Chang-Graham AL, Profeta LTM, Johnson TJ, Yokelson RJ, Laskin A, Laskin J. 2011. Case Study of
1022 Water-Soluble Metal Containing Organic Constituents of Biomass Burning Aerosol. *Environ. Sci.*
1023 *Techol.* 45:1257-63
- 1024 90. Fuzzi S, Baltensperger U, Carslaw K, Decesari S, van der Gon HD, et al. 2015. Particulate matter,
1025 air quality and climate: lessons learned and future needs. *Atmos. Chem. Phys.* 15:8217-99
- 1026 91. Quinn PK, Collins DB, Grassian VH, Prather KA, Bates TS. 2015. Chemistry and Related Properties
1027 of Freshly Emitted Sea Spray Aerosol. *Chem. Rev.* 115:4383-99
- 1028 92. George C, Ammann M, D'Anna B, Donaldson DJ, Nizkorodov SA. 2015. Heterogeneous
1029 Photochemistry in the Atmosphere. *Chem. Rev.* 115:4218-58
- 1030 93. Noziere B, Kaberer M, Claeys M, Allan J, D'Anna B, et al. 2015. The Molecular Identification of
1031 Organic Compounds in the Atmosphere: State of the Art and Challenges. *Chem. Rev.* 115:3919-
1032 83
- 1033 94. Zhang R, Wang G, Guo S, Zarnora ML, Ying Q, et al. 2015. Formation of Urban Fine Particulate
1034 Matter. *Chem. Rev.* 115:3803-55

- 1035 95. Wilson TW, Ladino LA, Alpert PA, Breckels MN, Brooks IM, et al. 2015. A marine biogenic source
1036 of atmospheric ice-nucleating particles. *Nature* 525:234-7
- 1037 96. Wang B, Harder TH, Kelly ST, Yancey Piens DS, China S, et al. 2015. Precipitation Generates
1038 Airborne Soil Organic Particles. *Nature Geoscience*:submitted
- 1039 97. Nie W, Ding A, Wang T, Kerminen V-M, George C, et al. 2014. Polluted dust promotes new
1040 particle formation and growth. *Scientific Reports* 4:6634
- 1041 98. Knippertz P, Stuetz J-BW, eds. 2014. *Mineral Dust, A Key Player in the Earth System*. Heidelberg
1042 New York London: Springer. 509 pp.
- 1043 99. Hallquist M, Wenger JC, Baltensperger U, Rudich Y, Simpson D, et al. 2009. The formation,
1044 properties and impact of secondary organic aerosol: current and emerging issues. *Atmos. Chem.*
1045 *Phys.* 9:5155-236
- 1046 100. Al-Abadleh HA. 2015. Review of the bulk and surface chemistry of iron in atmospherically
1047 relevant systems containing humic-like substances. *RSC Advances* 5:45785-911
- 1048 101. Jickells TD, An ZS, Andersen KK, Baker AR, Bergametti G, et al. 2005. Global iron connections
1049 between desert dust, ocean biogeochemistry, and climate. *Science* 308:67-71
- 1050 102. Hakkinen SAK, McNeill VF, Riipinen I. 2014. Effect of Inorganic Salts on the Volatility of Organic
1051 Acids. *Environ. Sci. Technol.* 48:13718-26
- 1052 103. Weller C, Horn S, Herrmann H. 2013. Photolysis of Fe(III) carboxylate complexes: Fe(II) quantum
1053 yields and reaction mechanisms. *Journal of Photochemistry and Photobiology a-Chemistry*
1054 268:24-36
- 1055 104. Weller C, Tilgner A, Braeuer P, Herrmann H. 2014. Modeling the Impact of Iron-Carboxylate
1056 Photochemistry on Radical Budget and Carboxylate Degradation in Cloud Droplets and Particles.
1057 *Environ. Sci. Technol.* 48:5652-9
- 1058 105. Elbert W, Taylor PE, Andreae MO, Pöschl U. 2007. Contribution of fungi to primary biogenic
1059 aerosols in the atmosphere: wet and dry discharged spores, carbohydrates, and inorganic ions.
1060 *Atmos. Chem. Phys.* 7:4569-88
- 1061 106. Sesartic A, Dall'Amico TN. 2011. Global fungal spore emissions, review and synthesis of literature
1062 data. *Biogeosciences* 8:1181-92
- 1063 107. Morris CE, Sands DC, Bardin M, Jaenicke R, Vogel B, et al. 2011. Microbiology and atmospheric
1064 processes: research challenges concerning the impact of airborne micro-organisms on the
1065 atmosphere and climate. *Biogeosciences* 8:17-25
- 1066 108. Despres VR, Huffman JA, Burrows SM, Hoose C, Safatov AS, et al. 2012. Primary biological
1067 aerosol particles in the atmosphere: a review. *Tellus B - Chem. Phys. Meteorol.* 64:15598
- 1068 109. Jaenicke R. 2005. Abundance of Cellular Material and Proteins in the Atmosphere. *Science*
1069 308:73
- 1070 110. Heald CL, Spracklen DV. 2009. Atmospheric budget of primary biological aerosol particles from
1071 fungal spores. *Geophys. Res. Lett.* 36:L09806
- 1072 111. Huffman JA, Sinha B, Garland RM, Snee-Pollmann A, Gunthe SS, et al. 2012. Size distributions
1073 and temporal variations of biological aerosol particles in the Amazon rainforest characterized by
1074 microscopy and real-time UV-APS fluorescence techniques during AMAZE-08. *Atmos. Chem.*
1075 *Phys.* 12:11997-2019
- 1076 112. Prenni AJ, Tobo Y, Garcia E, DeMott PJ, Huffman JA, et al. 2013. The impact of rain on ice nuclei
1077 populations at a forested site in Colorado. *Geophys. Res. Lett.* 40:227-31
- 1078 113. Spracklen DV, Heald CL. 2014. The contribution of fungal spores and bacteria to regional and
1079 global aerosol number and ice nucleation immersion freezing rates. *Atmos. Chem. Phys.*
1080 14:9051-9

- 1081 114. Schumacher CJ, Pöhlker C, Aalto P, Hiltunen V, Petäjä T, et al. 2013. Seasonal cycles of
1082 fluorescent biological aerosol particles in boreal and semi-arid forests of Finland and Colorado.
1083 *Atmos. Chem. Phys.* 13:11987-2001
- 1084 115. Martin ST, Andreae MO, Artaxo P, Baumgardner D, Chen Q, et al. 2010. Sources and properties
1085 of Amazonian aerosol particles. *Reviews of Geophysics* 48:RG2002
- 1086 116. Pummer BG, Bauer H, Bernardi J, Chazallon B, Facq S, et al. 2013. Chemistry and morphology of
1087 dried-up pollen suspension residues. *Journal of Raman Spectroscopy* 44:1654-8
- 1088 117. Griffiths PT, Borlace JS, Gallimore PJ, Kalberer M, Herzog M, Pope FD. 2012. Hygroscopic growth
1089 and cloud activation of pollen: a laboratory and modelling study. *Atmospheric Science Letters*
1090 13:289-95
- 1091 118. Grote M, Valenta R, Reichelt R. 2003. Abortive pollen germination: a mechanism of allergen
1092 release in birch, alder, and hazel revealed by immunogold electron microscopy. *Journal of*
1093 *allergy and clinical immunology* 111:1017-23
- 1094 119. Taylor P, Flagan R, Miguel A, Valenta R, Glovsky M. 2004. Birch pollen rupture and the release of
1095 aerosols of respirable allergens. *Clinical & Experimental Allergy* 34:1591-6
- 1096 120. Steiner AL, Brooks SD, Deng C, Thornton DC, Pendleton MW, Bryant V. 2015. Pollen as
1097 atmospheric cloud condensation nuclei. *Geophys. Res. Lett.*
- 1098 121. O'Sullivan D, Murray BJ, Ross JF, Whale TF, Price HC, et al. 2015. The relevance of nanoscale
1099 biological fragments for ice nucleation in clouds. *Scientific Reports* 5
- 1100 122. Després VR, Nowoisky JF, Klose M, Conrad R, Andreae MO, Pöschl U. 2007. Characterization of
1101 primary biogenic aerosol particles in urban, rural, and high-alpine air by DNA sequence and
1102 restriction fragment analysis of ribosomal RNA genes. *Biogeosciences* 4:1127-41
- 1103 123. Artaxo P, Rizzo LV, Brito JF, Barbosa HM, Arana A, et al. 2013. Atmospheric aerosols in Amazonia
1104 and land use change: from natural biogenic to biomass burning conditions. *Faraday Discuss.*
1105 165:203-35
- 1106 124. Meskhidze N, Petters MD, Tsigaridis K, Bates T, O'Dowd C, et al. 2013. Production mechanisms,
1107 number concentration, size distribution, chemical composition, and optical properties of sea
1108 spray aerosols. *Atmospheric Science Letters* 14:207-13
- 1109 125. Keene WC, Maring H, Maben JR, Kieber DJ, Pszenny AAP, et al. 2007. Chemical and physical
1110 characteristics of nascent aerosols produced by bursting bubbles at a model air-sea interface. *J.*
1111 *Geophys. Res. - Atmos.* 112
- 1112 126. Modini RL, Harris B, Ristovski ZD. 2010. The organic fraction of bubble-generated, accumulation
1113 mode Sea Spray Aerosol (SSA). *Atmos. Chem. Phys.* 10:2867-77
- 1114 127. Fuentes E, Coe H, Green D, McFiggans G. 2011. On the impacts of phytoplankton-derived
1115 organic matter on the properties of the primary marine aerosol – Part 2: Composition,
1116 hygroscopicity and cloud condensation activity. *Atmos. Chem. Phys.* 11:2585–602
- 1117 128. Prather KA, Bertram TH, Grassian VH, Deane GB, Stokes MD, et al. 2013. Bringing the ocean into
1118 the laboratory to probe the chemical complexity of sea spray aerosol. *Proc. Natl. Acad. Sci.*
1119 *U.S.A.* 110:7550-5
- 1120 129. Frossard AA, Russell LM, Burrows SM, Elliott SM, Bates TS, Quinn PK. 2014. Sources and
1121 composition of submicron organic mass in marine aerosol particles. *J. Geophys. Res. - Atmos.*
1122 119:12977-3003
- 1123 130. Quinn PK, Bates TS, Schulz KS, Coffman DJ, Frossard AA, et al. 2014. Contribution of sea surface
1124 carbon pool to organic matter enrichment in sea spray aerosol. *Nature Geoscience* 7:228-32
- 1125 131. Orellana MV, Matrai PA, Leck C, Rauschenberg CD, Lee AM, Coz E. 2011. Marine microgels as a
1126 source of cloud condensation nuclei in the high Arctic. *Proc. Natl. Acad. Sci. U.S.A.* 108:13612-7

- 1127 132. Ovadnevaite J, O'Dowd C, Dall'Osto M, Ceburnis D, Worsnop DR, Berresheim H. 2011. Detecting
1128 high contributions of primary organic matter to marine aerosol: A case study. *Geophys. Res. Lett.*
1129 38:L02807, doi: 10.1029/2010gl046083
- 1130 133. Facchini MC, Rinaldi M, Decesari S, Carbone C, Finessi E, et al. 2008. Primary submicron marine
1131 aerosol dominated by insoluble organic colloids and aggregates. *Geophys. Res. Lett.* 35:L17814
- 1132 134. Clarke AD, Owens SR, Zhou JC. 2006. An ultrafine sea-salt flux from breaking waves: Implications
1133 for cloud condensation nuclei in the remote marine atmosphere. *J. Geophys. Res. - Atmos.*
1134 111:14
- 1135 135. Pierce JR, Adams PJ. 2006. Global evaluation of CCN formation by direct emission of sea salt and
1136 growth of ultrafine sea salt. *J. Geophys. Res. - Atmos.* 111:16
- 1137 136. Collins DB, Ault AP, Moffet RC, Ruppel MJ, Cuadra-Rodriguez LA, et al. 2013. Impact of marine
1138 biogeochemistry on the chemical mixing state and cloud forming ability of nascent sea spray
1139 aerosol. *J. Geophys. Res. - Atmos.* 118:8553-65
- 1140 137. Wex H, Fuentes E, Tsagkogeorgas G, Voigtlander J, Clauss T, et al. 2010. The Influence of Algal
1141 Exudate on the Hygroscopicity of Sea Spray Particles. *Advances in Meteorology*:11
- 1142 138. Alpert PA, Kilthau WP, Bothe DW, Radway JC, Aller JY, Knopf DA. 2015. The influence of marine
1143 microbial activities on aerosol production: A laboratory mesocosm study. 120
- 1144 139. Ault AP, Zhao DF, Ebben CJ, Tauber MJ, Geiger FM, et al. 2013. Raman microspectroscopy and
1145 vibrational sum frequency generation spectroscopy as probes of the bulk and surface
1146 compositions of size-resolved sea spray aerosol particles. *PCCP* 15:6206-14
- 1147 140. Guasco TL, Cuadra-Rodriguez LA, Pedler BE, Ault AP, Collins DB, et al. 2014. Transition Metal
1148 Associations with Primary Biological Particles in Sea Spray Aerosol Generated in a Wave
1149 Channel. *Environ. Sci. Techol.* 48:1324-33
- 1150 141. Verdugo P. 2012. Marine Microgels. *Annual Review of Marine Science, Vol 4* 4:375-400
- 1151 142. Cisternas-Novoa C, Lee C, Engel A. 2015. Transparent exopolymer particles (TEP) and Coomassie
1152 stainable particles (CSP): Differences between their origin and vertical distributions in the ocean.
1153 *Mar. Chem.* 175:56-71
- 1154 143. Knopf DA, Alpert PA, Wang B, Aller JY. 2011. Stimulation of ice nucleation by marine diatoms.
1155 *Nature Geoscience* 4:88-90
- 1156 144. Alpert PA, Aller JY, Knopf DA. 2011. Initiation of the ice phase by marine biogenic surfaces in
1157 supersaturated gas and supercooled aqueous phases. *PCCP* 13:19882-94
- 1158 145. Sharoni S, Trainic M, Schatz D, Lehahn Y, Flores MJ, et al. 2015. Infection of phytoplankton by
1159 aerosolized marine viruses. *Proc. Natl. Acad. Sci. U.S.A.* 112:6643-7
- 1160 146. Donaldson DJ, George C. 2012. Sea-Surface Chemistry and Its Impact on the Marine Boundary
1161 Layer. *Environ. Sci. Techol.* 46:10385-9
- 1162 147. Zhou XL, Davis AJ, Kieber DJ, Keene WC, Maben JR, et al. 2008. Photochemical production of
1163 hydroxyl radical and hydroperoxides in water extracts of nascent marine aerosols produced by
1164 bursting bubbles from Sargasso seawater. *Geophys. Res. Lett.* 35:5
- 1165 148. Joung YS, Buie CR. 2015. Aerosol generation by raindrop impact on soil. *Nature Communications*
1166 6:6083
- 1167 149. O'Sullivan D, Murray BJ, Malkin TL, Whale TF, Umo NS, et al. 2014. Ice nucleation by fertile soil
1168 dusts: relative importance of mineral and biogenic components. *Atmos. Chem. Phys.* 14:1853-67
- 1169 150. Tobo Y, DeMott PJ, Hill TCJ, Prenni AJ, Swoboda-Colberg NG, et al. 2014. Organic matter matters
1170 for ice nuclei of agricultural soil origin. *Atmos. Chem. Phys.* 14:8521-31
- 1171 151. Wang BB, Knopf DA. 2011. Heterogeneous ice nucleation on particles composed of humic-like
1172 substances impacted by O(3). *J. Geophys. Res. - Atmos.* 116

- 1173 152. Koop T, Bookhold J, Shiraiwa M, Poeschl U. 2011. Glass transition and phase state of organic
1174 compounds: dependency on molecular properties and implications for secondary organic
1175 aerosols in the atmosphere. *PCCP* 13:19238-55
- 1176 153. Zhou S, Shiraiwa M, McWhinney RD, Poschl U, Abbatt JPD. 2013. Kinetic limitations in gas-
1177 particle reactions arising from slow diffusion in secondary organic aerosol. *Faraday Discuss.*
1178 165:391-406
- 1179 154. Vaden TD, Imre D, Beranek J, Shrivastava M, Zelenyuk A. 2011. Evaporation kinetics and phase
1180 of laboratory and ambient secondary organic aerosol. *Proc. Natl. Acad. Sci. U.S.A.* 108:2190-5
- 1181 155. Renbaum-Wolff L, Grayson JW, Bateman AP, Kuwata M, Sellier M, et al. 2013. Viscosity of alpha-
1182 pinene secondary organic material and implications for particle growth and reactivity. *Proc.*
1183 *Natl. Acad. Sci. U.S.A.* 110:8014-9
- 1184 156. Berkemeier T, Shiraiwa M, Pöschl U, Koop T. 2014. Competition between water uptake and ice
1185 nucleation by glassy organic aerosol particles. *Atmos. Chem. Phys.* 14:12513-31
- 1186 157. Pajunoja A, Lambe AT, Hakala J, Rastak N, Cummings MJ, et al. 2015. Adsorptive uptake of water
1187 by semisolid secondary organic aerosols. *Geophys. Res. Lett.* 42:3063-8
- 1188 158. Shiraiwa M, Yee LD, Schilling KA, Loza CL, Craven JS, et al. 2013. Size distribution dynamics reveal
1189 particle-phase chemistry in organic aerosol formation. *Proc. Natl. Acad. Sci. U. S. A.* 110:11746-
1190 50
- 1191 159. Donaldson MA, Bish DL, Raff JD. 2014. Soil surface acidity plays a determining role in the
1192 atmospheric-terrestrial exchange of nitrous acid. *Proc. Natl. Acad. Sci. U.S.A.* 111:18472-7
- 1193 160. Su H, Cheng Y, Oswald R, Behrendt T, Trebs I, et al. 2011. Soil Nitrite as a Source of Atmospheric
1194 HONO and OH Radicals. *Science* 333:1616-8
- 1195 161. Li Y, Pöschl U, Shiraiwa M. 2015. Molecular corridors and parameterizations of volatility in the
1196 evolution of organic aerosols. *Atmospheric Chemistry and Physics Discussion* 15:27877-915
- 1197